Theranostic Nanoparticles in Cancer Diagnosis and Treatment

Dipak Maity, Satya Ranjan Sahoo, Ankur Tiwari, Siddharth Ajith, and Sumit Saha

1 Introduction

Cancer (also known as malignancy) is a term for a group of diseases in which the body's cells multiply uncontrollably. This disease is one of the significant sources of death around the globe [1]. Nanoscience and nanotechnology provide immense potential to stop the spread of cancerous cells in the body. It helps to cure the disease in a specialized way at a nanoscale, thereby efficiently curing the disease. Till now, nanotechnology based cancer theranostics is in its initial stages of application but has a vast potential for research and development in the future. As the name suggests, theranostic is a combination of two words: therapy and diagnostics [2]. On a nanoscale, theranostic improves the diagnosis ability as well as efficiency of therapy [2]. Various theranostic nanomaterials have been evolved for cancer treatment and diagnosis, and it is discussed in a detailed way in this chapter. Due to their small size and high surface energy, nanomaterials react significantly with biomolecules in the cell [3].

D. Maity (✉)
Department of Chemical Engineering, University of Petroleum and Energy Studies, Dehradun, Uttarakhand, India

School of Health Sciences & Technology, University of Petroleum & Energy Studies, Dehradun, Uttarakhand, India

S. R. Sahoo · S. Saha
Materials Chemistry Department, CSIR-Institute of Minerals & Materials Technology, Bhubaneswar, Odisha, India

Academy of Scientific and Innovative Research (AcSIR), Ghaziabad, Uttar Pradesh, India

A. Tiwari · S. Ajith
Department of Chemical Engineering, Institute of Chemical Technology Mumbai-Indian Oil Campus, Bhubaneswar, Odisha, India

R. S. Chaughule et al. (eds.), *Nanomaterials for Cancer Detection Using Imaging Techniques and Their Clinical Applications*,
https://doi.org/10.1007/978-3-031-09636-5_7

The most significant advantage of using nanotechnology is its ability to deliver a targeted agent to the tumor site, which helps in the efficient treatment of the cancer disease. Nanotechnology also provides scientists and researchers with the opportunity to study the development of tumors even during their initial stages. Moreover, it is very essential to detect the tumors in their earlier stages for a proper cure for the cancer disease, which is easily possible using advanced nanotechnology [4]. The level of accuracy and precision that can be obtained by using nanotechnology is much better than the currently employed conventional techniques. Even though there are many advantages, there is also a chance of generating toxicity due to the nanomaterials, which must be researched further [4]. Nevertheless, the advancement of robust theranostic materials is one of the keys to discovering and treating cancer in the twenty-first century [3].

From this chapter, the reader can get a broad picture of the application of nanotechnology in the field of cancer therapy as well as about various theranostic nanomaterials which are investigated in cancer diagnosis and its treatment. Even though this modern technology has shown promising results in cancer theranostics, it has some limitations, which have also been discussed in this chapter. Almost all the aspects of theranostic nanomaterials have been considered, and one can conclude that nanotechnology is the future alternative for cancer treatment.

2 Classification of Theranostic Nanoparticles

Theranostic nanoparticles (TNPs) are multifunctional nanomaterials that are designed for specific and personalized disease management as they possess both diagnostic and therapeutic capabilities in a single biocompatible nanoparticle [5]. TNPs can ideally be those nanomaterials which can effectively accumulate and/or deliver the potential drugs selectively to the target site without affecting any other tissue/organ or the organism itself, are easily eliminated from the organism's body, and must be biodegradable into nontoxic by-products. In cancer treatment, TNPs have proved to be very attractive and promising agents [6]. They have the potential to revolutionize cancer treatment as they possess both the theranostics and drug delivery capability. In the last few decades, with the development of nanotechnology and nanoscience, there has been an increased interest in studies of various kinds of TNPs for simultaneous cancer imaging and therapy. These TNPs have been classified and discussed in detail in this section. A schematic representation of different TNPs used in cancer diagnosis and treatment is shown in Fig. 1.

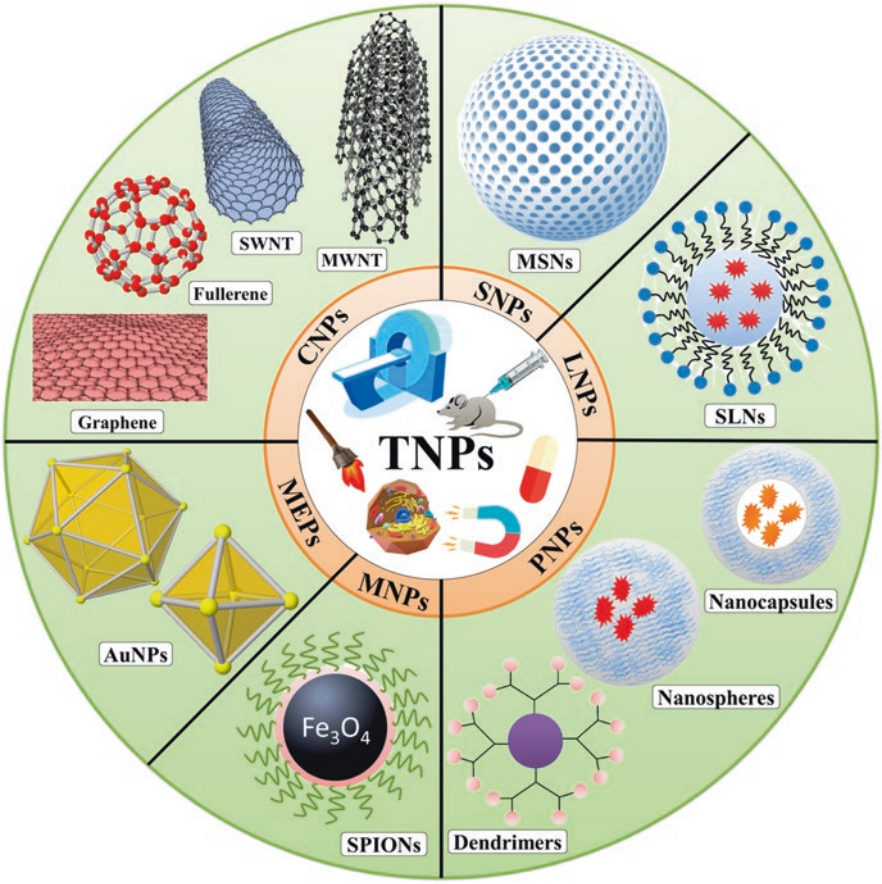

Fig. 1 Schematic representation of different TNPs used in cancer diagnosis and treatment

2.1 Magnetic Nanoparticles

Magnetic nanoparticles (MNPs) are considered one of the essential classes of nanomaterials that are widely studied for their potential application in theranostics and biomedicines. MNPs can be easily manipulated by an externally applied magnetic field, making them one of the important candidates for in vivo applications. MNPs are used in different applications like magnetic biosensing, magnetic imaging, drug delivery/targeting, hyperthermia therapy, etc. MNPs have a large surface-to-volume ratio and unique dissimilar magnetic behavior as compared to their bulk. Different materials like pure metals (Fe, Co, Ni, etc.), alloy (Fe-Pt), and oxides/ferrites (like Fe_3O_4, γ-Fe_2O_3) are commonly used MNPs in nanomedicine. However, pure metals are not suitable for clinical application owing to their toxicity and rapid oxidation tendency. Iron oxide is widely used in the fabrication of MNPs as it is chemically stable, nontoxic, non-immunogenic and biodegradable

[7]. Hence, iron oxide nanoparticles like magnetite (Fe_3O_4) and maghemite (γ-Fe_2O_3) are commonly used MNPs in biomedical applications due to the fact that these MNPs have higher effective areas, improved tissular diffusion, and reduced magnetic dipole-dipole interactions. Additionally, their particle size is smaller enough to circulate through the capillary system of organs and tissues. Nevertheless, their movement can be controlled by magnetic fields as they have high magnetization and can be immobilized close to the target pathogenic tissue [8].

Superparamagnetic iron oxide nanoparticles (SPIONS) are a type of MNPs that display unique superparamagnetic properties as compared to ferro−/ferrimagnetic iron oxide nanoparticles in the presence of an external magnetic field. They have various biomedical applications such as magnetic fluid hyperthermia, MRI, drug delivery, and gene delivery due to their exceptional physicochemical characteristics: magnetic properties, chemical stability, biodegradability, and low toxicity. Generally, the SPIONS have a core-shell structure of magnetite and/or maghemite cores with a surface coating of nonmagnetic organic/inorganic species which prevents the SPIONs from aggregation. These stabilizing coatings play an essential role in determining magnetic and physicochemical properties of the SPION core. Coercivity of the multi-domain MNPs gradually increases with reducing their size and reaches to the maximum at their single-domain size, and subsequently decreases to zero with further reducing their size up to superparamagnetic size. Therefore, SPIONs reveal superparamagnetism behavior (i.e., zero coercivity and remanence) below their superparamagnetic size limit. Moreover, these particles exhibit high saturation magnetization and magnetic susceptibility under the influence of an externally applied magnetic field [9].

2.2 Carbon-Based Nanoparticles

Carbon-based nanoparticles (CNPs) are entirely made up of carbon. Carbon has many allotropic forms like graphite, diamond, and amorphous carbon. CNPs have sp^2-hybridized carbon atoms that have been developed in various dimensions. Different carbon-based nanomaterials can be classified as follows:

1. Fullerene (zero dimensional), a hollow cage-like structure. They are made up of sp^2-hybridized carbon atoms. Its structure is similar to hollow football with pentagonal/hexagonal carbon units organized in a regular pattern. Most of the fullerenes are spheroids in shape (like C_{60}). However, oblong shapes like Rugby balls also exist (like C_{70}). Fullerenes are an allotrope of carbon. They have unique photophysical and photochemical properties, and also good electrical conductivity, and higher strength.
2. Carbon nanotubes (CNTs) (one dimensional), which is structurally one carbon atom thick sheet rolled into hollow elongated tubes having 1 nm of diameter. The carbon atoms are linked in a hexagonal structure. Based on rolling, CNTs can be categorized into single-walled CNTs (SWNTs) and multi-walled CNTs

(MWNTs). In SWNTs, the sheets are single-rolled, whereas MWNTs consist of multiple rolled sheets. Each layer in MWNTs interacts through van der Waals forces. CNTs have high tensile strength, good electrical and thermal conductivity, optical properties, and mechanical properties.

3. Graphene sheets (two dimensional) are allotropic forms of carbon composed of sp^2-bonded carbon atoms that form a hexagonal network of honeycomb lattice in two-dimensional planar surfaces. Generally, the thickness of graphene sheets is 1 nm. The various derivatives of graphene include graphene oxide, reduced graphene oxide, chemically modified graphene oxide, etc. They have unique properties like high electrical conductivity, good chemical stability, large surface area, etc.
4. Graphite and nanodiamonds (three dimensional) are made up of sp^2 carbon atoms arranged in a hexagon sphere, and nanocrystals consisting of tetrahedrally bonded carbon atoms, respectively. Nanodiamonds (NDs) have unique optical properties. Besides, there are also other forms of carbon-based nanomaterials like carbon quantum dots, carbon nanofibers, and carbon black.

CNPs have excellent mechanical, thermal, optical, and chemical properties. With these properties, they also have unique structural dimensions that make them be utilized in widely diverse areas of applications of which biomedical application is very significant. In recent times, CNPs have been utilized in the imaging of cells and tissues and the delivery of therapeutic molecules for different diseases. Moreover, due to the broad one-photon property of CNPs, they have been recently used as imaging agents in tumor diagnosis. The intrinsic two-photon fluorescence property in the long-wavelength region helps in deep tissue optical imaging [10]. Further, CNPs have an internal structure based on graphene sheets assembled to form quasi-spherical nanoparticles, and the external shell can be functionalized with different functional groups. They also show a peculiar optical property, particularly in the UV-Vis spectrum, where it shows a broad range of absorption bands and a tail in the UV and visible regions, respectively. This is due to π-π^* and n-π^* transitions related to C=C and C=O, respectively [11].

2.3 Silica-Based Nanoparticles

Silica-based nanoparticles (SNPs) are colloidal silica (silicon dioxide) nanoparticles that are amorphous and generally spherical. They have different ranges of sizes with different surface chemistry. There are two major types of SNPs, namely, solid silica nanoparticles (SiNPs) and mesoporous silica nanoparticles (MSNs) [12]. Both have different properties. SiNPs have favorable colloidal properties and are photochemically stable. Being biocompatible, the surface of SiNPs can be functionalized (with various functional groups like antibodies, aptamers, and polymers) to be utilized as an optical imaging and drug delivery agents. Further, MSNs have a

high surface area and tunable pores that can be utilized for loading therapeutic or imaging agents.

SNPs are classical types of materials which are largely used in biomedical applications as they are inexpensive and it is very easy to prepare. Their surface characteristics, porosity, and functionalization can be tuned to make them good tools for biomolecule detection and separation (like protein adsorption and separation, nucleic acid detection and purification) and provide a suitable medium for drug delivery, gene delivery, and imaging [13]. Since they are biocompatible, they are typically designed to be used as nanocarriers and/or biomodulators for therapeutic delivery [14]. Moreover, SNPs, especially the porous variant (i.e., MSNs), can be an excellent tool for antimicrobial drug delivery agents due to their high drug loading capacity, tunable pore size and volume, ease of functionalization, and biocompatibility [15]. Besides, SNPs are chemically inert, and their matrix porosity is not susceptible to swelling or change in pH. Therefore, it can be used to encapsulate theranostic agents like photosensitizers, and it can also selectively accumulate in cancer cells for effective cancer treatment (like improving efficacy of photodynamic therapy). Furthermore, SNP surfaces can be easily functionalized or modified with cancer specific biomolecules for tumor cell targeting [16].

2.4 Metallic Nanoparticles

Metallic nanoparticles (MEPs) are generally nanoscale metals whose dimensions lie within a range of 1–100 nm. Faraday, in 1857, was the first to recognize the existence of metallic nanoparticles in solution, and Mie, in 1908, gave the quantitative explanation of their color [17]. In recent years with the development of nanotechnology and nanoscience, MEPs have received enormous attention and increased interest for studies due to which it has been exploited in different application fields, especially in biomedical fields. MEPs have various shapes, tunable surface chemistry/surface functionalization, unique optical properties (like surface plasmon resonance), versatile functionalization, and a good penetration with traceability in the living organism, which makes them be utilized as an excellent theranostics agent in cancer treatment. MEPs generally have a small size of about 50 nm, enabling them to cross or penetrate the capillaries in tissues and cells and thus reach the targeted area. Moreover, they have a high surface/volume ratio with the modified surface, allowing them to carry many potential drugs as a drug carrier and thus help in drug delivery. One of the unique advantages of using MEPs in cancer treatment is that they can efficiently absorb light and convert it to heat. This makes them be used in hyperthermic tumor therapy in which photo stimulation provides thermal energy, which makes this therapy highly specific.

Considering their inherent CCT, PA, fluorescence, surface-enhanced Raman scattering (SERS), and PTT imaging properties, MEPs, particularly Ag and Au have mainly focused on cancer theranostics. In order to improve their biocompatibility and avoid RES uptake, the surfaces of MEPs have been modified with various

molecules (e.g., PEGylated). A significant advantage of MEPs is that they can be functionalized with tumor-specific ligands and stimuli-responsive components and be conjugated with other therapeutic/imaging agents to achieve targeted/triggered delivery and multimodal cancer theranostics [18].

2.4.1 Silver Nanoparticles

Silver has been extensively used in coins and jewelry due to its noble properties like gold since ancient history. Silver is also resistant to bacteria and is thus used as an antibacterial agent with low toxicity. Hippocrates (considered to be the father of modern medicine), known for his outstanding figures in the history of medicines, believed in the healing effect of silver because of its anti-disease properties. Because of this healing effect, it was used to protect water. Silver compounds had been used in curing wound infections instead of antibiotics during World War I. In today's era of nanotechnology and nanoscience, new theranostics approaches have been developed by which silver nanoparticle (AgNPs) is used as medicines. AgNPs are extensively used in industrial and health products, like coating medical devices; biosensors; bioimaging; antibacterial, antifungal, antiparasitic, antiviral, anticancer agents; and drug carriers and therapeutics [19]. The reasons behind its extensive use are its superior physicochemical characteristics, which include high conductivity, better plasmonic properties, and chemical stability, as well as its antibacterial, antiviral, and antifungal properties.

2.4.2 Gold Nanoparticles

Gold is one of the oldest metals, which was discovered several thousand years ago. It is one of the least reactive chemical elements, making it resistant to corrosion and other chemical reactions. The unique bright yellow color of gold made it be used for coinage and jewelry. Thus, gold became the symbol of power and wealth. Ancient Chinese, Arabian, and Indian papers from fifth to fourth centuries BC reported the medicinal application of gold and its complexes which recommended it to treat various diseases. In 1857, Faraday presented the first scientific article on gold nanoparticles, a red colloidal, and described its light scattering features. Like AgNPs, gold nanoparticles (AuNPs) are also extensively used in cancer theranostics due to their unique physicochemical properties like surface plasmon resonance (SPR) and ability to bind with amine and thiol group, which allows surface modification so that it can be used in biomedical applications [20]. Further, AuNPs display tunable physicochemical properties due to their different sizes (2–100 nm) and shapes, including nanospheres, nanorods, nanoshells, nanocages, nanostars, and surface plasmon resonance (SPR) properties, along with tailor-made surface functionalization. As a result, they are extensively used in several single-modal theranostics applications, including optical−/photoacoustic-/CT-imaging of cancer cells, PTT, and anticancer drug delivery [18].

2.5 Polymer Nanoparticles

Polymer nanoparticles (PNPs) are composed of polymers that are prepared by simply converting monomers or bulk polymers to nano-sized polymers. It can be defined as those solid colloidal particles in the range of 10–1000 nm which can be loaded with active compounds on the surface or inside the polymer core. The term "polymer nanoparticles" is collectively used for all types of nano-sized polymer particles, but specifically for polymer nanospheres and nanocapsules [21]. Polymer nanospheres are matrix particles where the entire mass is solid, and molecules are adsorbed at the surface of the sphere or encapsulated within the matrix particles. Whereas nanocapsules are vesicular reservoir systems, which have a liquid core surrounded by a solid material shell that is made up of a continuous polymeric network. Inside the liquid core, usually biologically active molecules (like drugs, genes, nucleic acid, etc.) are dissolved/encapsulated.

In the preparation of PNPs, both natural and synthesized polymers are used. However, natural polymers are more preferred owing to their biodegradability. Thus, natural polymers are used to make polymer nanoparticles for in vivo drug delivery systems. Examples of such natural polymers used for the preparation of PNPs are starch, polypeptides, albumin, polyhydroxyalkanoate (PHAs), gelatin, cellulose, etc. On the other hand, Synthetic polymers used in the preparation of nanoparticles are polyethylene (PE), polyethylene glycol (PEG), poly lactic-co-glycolic acid (PLGA), and polyvinyl alcohol (PVA) [22]. PNPs can be produced by various techniques. Generally, there are two main strategies to prepare PNPs, namely, the dispersion of performed polymer and the direct polymerization of monomers [23].

Further, surfaces of PNPs are often functionalized with different functional groups like surfactant, metal ions, or small molecules for better binding, targeting, and delivery purpose. By converting polymer to PNPs induces unique physicochemical properties. Moreover, due to their small size, high volume to surface area ratio, and tunable pore, polymer nanoparticles are extensively used for various applications like biosensors, drug delivery, stimuli response cargo delivery, and agricultural and environmental applications. The advantage of using PNPs in drug delivery systems includes high drug encapsulation efficiency, high stability, ability to protect drugs, and biocompatibility with tissue and cells. In fact, today, nanotechnology and nanoscience are employed to design such polymer nanoparticles that can effectively and efficiently deliver the drug to the target site and increase the therapeutic effect.

2.6 Lipid Nanoparticles

Structurally, lipids broadly consist of a nonpolar hydrophobic "chain" or "tail" region attached to the polar hydrophilic "head" region. Based on their structure, lipid-based nanoparticles can be classified into liposomes, lipid nano-emulsions (LNEs), solid lipid nanoparticles (SLPs), and nanostructured lipid carriers (NLCs). Liposomes are mainly composed of phospholipids arranged in bilayer structure to form "unilamellar vesicles" in the presence of water due to their amphipathic properties. These vesicles can be used to load drugs and carry them to the target area, thus improving drugs' solubility and stability. They are capable of encapsulating either hydrophobic or hydrophilic drugs. LNEs consist of lipid droplets stabilized by surfactants/phospholipids to prevent them from aggregation and coalescence in an aqueous solution. LNEs are somewhat like liposomes except that the outer phospholipid bilayer structure is absent, and instead, they exhibit a complex micelle-like structure of cationic lipids that encapsulate various oligonucleotides (like RNA and DNA). SLPs are a colloidal system made up of lipids that are solid at room temperature. The solid lipid forms a matrix material that acts as nanocarriers by encapsulating the drug and the matrix is stabilized by a mixture of surfactants or polymer. NLCs are the second generation of lipid-based nanocarriers developed from SLNs due to their limitations, such as lower drug loading efficiency and drug explosion due to its crystallization during storage. NLCs are formed by mixing solid and liquid lipids such as glyceryl tricaprylate, ethyl oleate, isopropyl myristate, and glycerol dioleate. Mixing solid lipids with small amounts of liquid lipids produces NLCs whose matrix is structurally rearranged concerning SLPs, which gives improved properties but at the same time maintains the benefits of SLPs [24].

2.7 Dendrimers

Dendrimers are polymerlike nanoparticles, but structurally they are different from PNPs. The word dendrimer is derived from the Greek word known as "dendron" whose literal meaning is "branching of a tree." Dendrimers are nano-sized polymeric globular branched and symmetrical structures with a size that varies from 1 to 15 nm [25]. Besides, dendrimers have well-defined, homogenous, and mainly monodisperse structures containing treelike branching units growing around a small molecule or polymer core. These branching units can be functionalized with various functional groups (like COOH, COONa, NH_2, or OH) that determine the physicochemical or biological properties of the dendrimers. Dendrimers have unique biological properties such as polyvalency, self-assembly, electronic interactions, chemical stability, low toxicity, and solubility, making them suitable for medical field applications, especially cancer treatment. Dendrimers can carry large amounts of drugs to a specific site and they can be considered as an architectural motif but not as a chemical compound [26]. A variety of dendrimers exists, among which

PAMAM (polyamidoamine) are the most common class of dendrimers and also most employed ones, especially in biotechnological applications, although PPI (polypropylene imines) are the first dendrimers to be reported. Further, they are biocompatible and non-immunogenic, making them a good candidate for drug delivery. PAMAM has the inner core made up of alkyl-diamine with tertiary amine branches surrounding the core.

3 Synthesis of Nanoparticles

With the development of nanotechnology, several synthetic routes have been developed to achieve desired physical and chemical properties in the fabricated nanomaterial. Broadly speaking, there are two synthetic approaches which are identified as (i) top-down approach (ii) bottom-up approach. Both approaches have their own advantages and disadvantages. The top-down approach (destructive approach) begins with a suitable bulk material (as starting material) and then trimming down/breaking down into smaller molecules, and then these smaller molecules are transformed into desired nanoparticles. The bottom-up approach is the reverse of the top-down approach. In the bottom-up approach (constructive approach), nanoparticles are first obtained at the atomic level by miniaturization of material and then by the integrating/self-assembly process, which leads to the formation of nanostructures. During self-assembly, the physical forces operating at nanoscales are used to combine the units: atom by atom, molecule by molecule, and/or cluster by cluster into larger stable nanostructures.

The basic synthetic methods involved in preparing nanomaterials are physical and chemical methods which are basically top-down and bottom-up approaches, respectively. There are also biological methods for synthesizing nanoparticles in which different microorganisms and plant parts are used to prepare nanomaterials. Each method has its own advantages and disadvantages and impacts various properties on the nanomaterial. The procedures used for the synthesis of nanoparticles have been discussed in detail. The methods of synthesis of nanoparticles are summarized in Table 1.

3.1 Physical Methods

3.1.1 Pulse Laser Ablation

Pulse laser ablation is one of the simplest and most common synthetic techniques of nanoparticles from different solvents. The technique consists of a solid disc that rotates with a solution that is placed in a vacuum chamber. The disc is exposed to a high-power pulsed laser beam. The laser beam enters the chamber and hits the targeted disc where the material is placed. The material, when exposed to such

Table 1 Classification, composition, methods of synthesis, and size of nanoparticles with their cancer theranostics applications

Classification	Composition	Method of synthesis	Size	Applications	References
Magnetic nanoparticles	Fe_3O_4, γ-Fe_2O_3	Coprecipitation Microemulsion Hydrothermal Thermal decomposition	1–100 nm	MRI, hyperthermia therapy, MPI	[54–59]
Carbon-based nanoparticles	sp^2-hybridized carbon atoms	Hydrothermal Laser ablation CVD	3–10 nm	Targeted drug delivery, PDT, thermal therapy	[60–65]
Silica-based nanoparticles	Colloidal silica (silicon dioxide)	Microemulsion Stober method	10–500 nm	Fluorescence imaging, targeted drug delivery	[66–70]
Lipid-based nanoparticles	Cholesterol and glycerophospholipid	Microemulsion	50–1000 nm	Functionalization of nanoparticles, targeted drug delivery	[71–73]
Polymer-based nanoparticles	Polymers in nanoscale	Microemulsion Nanoprecipitation Solvent evaporation	10–1000 nm	Multimodal imaging, targeted drug delivery	[74–77]
Metal nanoparticles	Pure metal (e.g., gold, silver, platinum, zinc, iron) or their compounds (e.g., oxides, hydroxides, sulfides, chlorides)	Biological methods Thermal decomposition Coprecipitation Hydrothermal Sputtering	10–100 nm	PDT, thermal therapy, targeted drug delivery, a contrast agent (PA imaging, MRI, fluorescence imaging)	[78–82]

high-power laser radiations, is converted to plasma to produce nanoparticles [27]. Many factors affect the final product, such as type of laser, number of pulses, pulsing time, and type of solvent. Stable nanoparticles are usually synthesized using pulse laser ablation techniques that do not require stabilizing agents or chemicals.

3.1.2 Electron Beam Lithography

Originally lithography has been utilized since the seventeenth century in the application of ink printing. Lithography is the process of transferring a pattern from one media to another. In today's era of nanotechnology and nanosciences, the technique and application of lithography are diversified toward the synthesis/fabrication of nanomaterials. The process of lithography involves patterning on a surface through the exposure of light, ions, and electrons, and subsequently, it etches or deposits the material on the surface to produce the pattern. There are different types of nanolithography techniques such as optical, electron beam, multiphoton, nanoimprint, and

scanning probe lithography [28]. The main advantages of nanolithography are that it can produce a single nanoparticle to a cluster with desired shape and size and the disadvantages that it requires complex equipment which has a high cost with it [29].

Electron beam lithography came into the picture by the late 1960s by modifying the design of SEM. This lithographic technique has the capacity to create patterns at the nanoscale because of its very short wavelength and reasonable electron density characteristics. The process involves electron irradiation of a surface that is covered/coated with an electron-sensitive material (resist) by a focused electron beam. Due to the irradiation, energetic absorption in specific places leads to an intramolecular phenomenon. Electron beam lithography consists mainly of three steps: exposure of the sensitive materials, development of the resists, and pattern transfers. The working principle of electron beam lithography is quite simple. A focused beam of electrons is irradiated on a substrate covered by an electron-sensitive material that changes its solubility properties according to the energy impacted by the electron beam. A typical electron beam lithography system closely resembles an SEM. A typical electron beam lithography setup consists of a chamber, electron gun, and column. Column and chamber are maintained in a high vacuum. The column contains electron-optical elements, which are used to create a beam of electrons and accelerate it, turn it on/off, and focus/deflect [30].

Electron beam resists are generally coated on the substrate to record an image of the pattern to be transferred. These resists are usually high molecular weight polymers that are dissolved in a suitable liquid solvent. When a focused electron beam is irradiated on these polymers, they undergo structural changes. Polymethyl methacrylate (PMMA) is the most commonly used electron resist. It is dissolved in solvents like anisole and chlorobenzene of the desired concentration. This technique synthesizes AuNPs; for instance, Lennox et al. prepared 2D patterned arrays of AuNPs by electron beam lithography [31].

3.1.3 High-Energy Ball Milling

High-energy ball milling is a solid processing technique used to synthesize nanoparticles. It is an inexpensive method to get the nanoparticle from the bulk. The starting bulk material can be of any shape/size. There are many types of milling, such as planetary, vibratory, rod, tumbler, etc. In this process, the powder mixture of the material is placed in a ball mill and subjected to high-energy collisions from the balls by which a vast brute force is applied to the materials. The ball is placed in a container that is closed with tight lids. During the grinding process, it decreases the particle size and produces micro deformation in the crystal lattice of the ground materials. Usually, a ratio of 2:1 by mass of balls to the material is maintained. Sometimes the container is filled with inert gas to prevent it from air contamination [32]. Impurities from the balls may get added—the temperature rises during the collision for which cryo-cooling is used to dissipate the heat generated. During milling, liquids are also used. Sometimes more than one container is used at a time to

prepare large amounts of fine particles. The balls are made up of hardened steel or tungsten carbide.

The mechanical limitation of this process is that ultrafine particles are either difficult to produce or take a long time. However, the simple operation, low cost, and large-scale production of nanoparticles are the main advantages of high-energy ball milling. The final product from this process depends on factors like the type of mill, milling speed, milling time, container, temperature, atmosphere, size and size distribution of the grinding material, process control agent, extent of filling of the container, and ratio by mass of ball to the material.

3.2 Chemical Methods

3.2.1 Coprecipitation Method

Coprecipitation is a very convenient method for synthesizing various nanoparticles such as, iron oxide nanoparticles. The coprecipitation method involves the simultaneous occurrence of conversion of the reactant into solution in their insoluble form followed by nucleation and growth [33]. The precipitation of a crystalline solid occurs in three steps: supersaturation, nucleation, and growth. During supersaturation, the system is unstable, and the precipitation of the product pieces occurs due to any small perturbation. Supersaturation is reached by various physical means like changing temperature or solvent evaporation, etc., and chemical means like the addition of acid, base, etc. These supersaturation conditions are necessary for inducing precipitation. Nucleation is the crucial step that involves the formation of small elementary particles of a new phase that are stable under precipitation conditions. Nucleation is followed by growth or agglomeration of the particle where crystal growth occurs, which affects the size, morphology, purity, and properties of the products. If the rate of nucleation is much higher than the rate of crystal growth, a large number of small particles will be formed, which leads to the formation of an amorphous precipitate. These techniques mostly prepare hydroxide and carbonate due to low solubility [34].

MNPs can be conveniently prepared by the coprecipitation method. Massant in 1981 reported the synthesis of MNP in acid and alkaline media. Since then, it is still used to prepare MNPs like iron oxide. In this technique, an aqueous solution of ferric and ferrous (Fe^{3+} & Fe^{2+}) ions is reduced by a basic solution at a temperature below 100 °C to form a precipitate. The advantages of coprecipitation are high yield, high product purity, organic solvent not used, and low cost [33].

3.2.2 Chemical Vapor Deposition

Chemical vapor deposition (CVD) is a powerful technique for producing high-quality, high-performance solid materials by a chemical reaction in the vapor phase. In a typical CVD method, the heated substrate (wafer) is exposed to one or more volatile precursors, which decompose on it, followed by deposition of a thin film on the substrate. This deposition is carried out in a reaction chamber. The vaporized precursor, along with combining gas, is transported in a CVD reactor where the substrate is kept at a high temperature. The reactant diffuses to the surface of the substrate and undergoes some chemical reaction, nucleates, and grows to form a thin film of the desired material. The by-product formed during the chemical reaction is removed by gas flow through the reactor [35]. It is widely used in the industry for producing thin-film semiconductors. There are many types of CVD like metallo-organic CVD (MOCVD), atomic layer epitaxy (ALE), vapor phase epitaxy (VPE), plasma-enhanced CVD (PECVD), etc. The advantage of CVD is that highly pure potent, and this technique can produce hard nanoparticles. The disadvantages of this technique are that it requires specialized equipment and the gaseous by-products formed are highly toxic and corrosive. A typical CVD system consists of a gas delivery system, a reaction chamber, a vacuum system, an energy system, an exhaust gas treatment system, and an automatic control system [36].

3.2.3 Microemulsion

The emulsion is the liquid-liquid dispersion of two immiscible liquids. They are mixed by mechanical shear and surfactant. The particle grows continuously with time, and hence it gets separated by gravitational forces. Thus, emulsions are thermodynamically unstable. Depending on the size of the droplet, emulsions are categorized as macro-emulsions, mini-emulsions, and microemulsions. Microemulsions (as defined by IUPAC) are dispersions made of water, oil, and surfactant that are isotropic and thermodynamically stable with dispersion droplets of size 1–100 nm (approximately). The microemulsion method is one of the low-temperature routes for the synthesis of nanoparticles. J.H Schulman first coined it in 1959 [37]. The microemulsion synthesis method is widely used for synthesis in inorganic nanoparticles. Nanoparticles can be produced in a controlled manner through the use of microemulsions, which are self-aggregated colloidal systems. Thus, in this method, control over the shape, size, and morphology of metallic nanoparticles is achieved by which we get different shapes and sizes of nanoparticles by just controlling the reaction time, temperature, and other reaction conditions.

When water and oil are mixed, they get separated into two phases due to the interfacial tension between them. This interfacial tension can be avoided by using a surfactant as it has hydrophilic and lipophilic groups that get aligned at the interface of water and oil, thus establishing an interaction between water and oil. There are various categories of microemulsion, like water in oil (W/O) microemulsion where water is dispersed in oil and oil in water (O/W) microemulsion where oil is

dispersed in water. Water in supercritical CO_2 microemulsion is also a kind of microemulsion that was recently developed. Among them, W/O microemulsion is essential as it is used to synthesize inorganic nanoparticles. They are usually called reverse micelles. This reverse micelle acts as nanoreactors. Preparation of metallic nanoparticles in W/O microemulsion usually involves mixing of two microemulsions containing metal salt and a reducing agent, respectively. On mixing the microemulsions, Brownian motion is formed, which results in the collision of reverse micelles. During this collision, an exchange of reaction occurs between two reverse micelles (nanoreactors). After a successful collision, intermicellar exchange of reactant takes place, and thus nucleation starts with a good growth process around the nucleation point [38]. Thus, a good collision is essential for coalescence, mixing of reaction, nucleation, and growth of nanoparticles. Therefore, factors controlling the structure and dynamics of these nanoreactors can be easily manipulated to control the nanoparticles' morphology, size, shape, and composition. Surfactants stabilize these particles and prevent them from growing.

3.2.4 Hydrothermal Method

In the solvothermal process, the chemical reaction occurs in a sealed vessel (known as autoclave) where the temperature is above the boiling point of the solvents used during the chemical reaction. If the solvent used is water, then the process is called the hydrothermal process. In the past, the hydrothermal method was used to study the formation of rocks and minerals. The hydrothermal process was utilized in crystal formation and growth, and in today's era of nanotechnology and nanoscience, it has been used to prepare various NPs. Its simple synthetic process, low cost, effective crystal growth, and convenient operation from solution make it a convenient method for producing nanostructure. Hydrothermal is a subset of solvothermal methods, which has the advantage of being safe and environmentally friendly because it involves water as a solvent for crystal growth instead of organic solvents [39].

Basically, in hydrothermal processes, the species which are poorly or insoluble under normal conditions are dissolved and recrystallized under high temperature and high pressure. The primary step in the hydrothermal process is crystalline growth which can be achieved by the following steps:

1. The reactants are first dissolved in the hydrothermal medium to form ions.
2. Due to the temperature difference in the upper and lower region in an autoclave, the ions are separated. These ions are transported to the low-temperature region, where seed crystals are grown to form a supersaturated solution.
3. Finally, crystal growth occurs, and thus crystallization occurs. The morphology of the crystals grown in this process depends on the growth conditions. This process allows the size, shape, and crystallization control by altering some parameters like growth temperature, reaction time, a precursor used, etc.

Water has a very crucial role in the hydrothermal process. As we know, water's viscosity and surface tension decrease with increases in temperature. Therefore, in a hydrothermal system, the viscosity of water decreases, and the mobility of ions increases, and also, due to an increase in vapor pressure in the hydrothermal system, the mobility of ions increases which accelerates the reaction by the increase in the number of collisions. Therefore, collectively all these phenomena favor the growth of crystals [40].

A wide variety of nanomaterials have been fabricated by this hydrothermal technique using the microwave, mechanical mixing, and electric field to enhance the productivity and efficiency of the process. However, the microwave based hydrothermal mechanism has been gathering more attention by researchers in recent years.

3.2.5 Thermal Decomposition

Thermal decomposition is chemical deposition that is caused by heat. The endothermic reaction breaks the chemical bonds and splits them into smaller ones. Each element has a specific temperature at which it decomposes. The nanoparticles are produced by decomposing the metals at that specific temperature [34]. Thermal decomposition is a unique way to synthesize monodispersed metalic nanoparticles. The size and shape can easily be controlled by manipulating various factors like concentration and type of reactant/precursor, stabilizing/capping agents, temperature, duration of reaction, etc.

Coordinate compounds like organometallic precursors are commonly used in thermal decomposition method as they give high-quality monodispersed metalic nanoparticles. Thermal decomposition of coordinate compounds carried out in presence of stabilizing agents and reducing agents to reduce the metallic ions of the coordination compounds. Generally, surfactants are used as stabilizing agents to stabilize the nanoparticles formed by reducing agents. They are also called capping agents. During thermal decomposition, the reduced species are treated with these capping agents at a particular temperature. Some other examples of capping agents are thiols, carboxylic acids, amines, etc. The suitable temperature at which thermal decomposition will occur is dependent on the nature of metal ions and ligands in the coordination compounds. After thermal decomposition, the product is dissolved in polar/nonpolar solvents like ethanol, hexane, toluene and deionized water. Then, the whole solution is centrifuged to separate the colloidal nanoparticles. It is redispersed in a polar/nonpolar solvents and washed for several times to purify the nanoparticle. Finally, the nanoparticles are dried after washing [41].

3.3 Biological Methods/Green Synthesis Methods

The biological methods for the synthesis of nanoparticles involve plant extracts and microorganisms. Plants, bacteria, fungi, yeast, algae, and viruses have been used to produce low-cost, energy-efficient, nontoxic metallic nanoparticles by various promising biological approaches [42]. Unlike chemical methods, it does not involve toxic chemicals; instead, it is a commonly used green approach for synthesizing nanoparticles as it is cheap, eco-friendly, and can be scaled up to a large scale. It does not involve harsh conditions like high temperatures, high pressure, and very sophisticated and high-cost instruments. Actually, the biological method of synthesis results from the overlap of nanotechnology and biotechnology. Scientists and researchers are increasingly showing interest in this nanoparticle synthesis technique because of its economic viability and ecofriendliness. It is easier to tailor the size, shape, and morphology by just modifying the culture conditions like pH, temperature, and nutrients. Biological species and inorganic materials have a particular interaction from the origin of life. These regular interactions have sustained life on this planet. Researchers have utilized these unique interactions to synthesize nanoparticles from biological entities like plant extracts and microorganisms. They used plant extracts and microorganisms as bio-reductants to reduce metal ions to produce nanoparticles and also as stabilizing agents without using any other additional agents [43].

3.3.1 By Plants

In recent years, phyto-nanotechnology has emerged as a new field to synthesize nanoparticles and apply nanotechnology in the plant system. Due to such increased attention, plants and their extracts have been exploited to synthesize nanoparticles. Different types of plants and their various parts, such as leaf, stem, bark, fruit, etc., have been used to synthesize nanoparticles because of their excellent phytochemical contents it has [44]. Therefore, plants are righteously called chemical factories of nature. These phytocompounds extracted from plants, namely, terpenoids, alkaloids, flavonoids, steroids, phenols, and enzymes, play an essential role in synthesizing nanoparticles as they act as both bio-reductant and stabilizing agents. Biomolecules extracted from plants reduce metal in a single step. This reduction can be easily conducted at room temperature and pressure, which can be easily scaled up [45]. Many nanoparticles like silver gold, palladium, platinum, ZnO, TiO_2, etc. are synthesized by the plat extract-mediated process [46–49].

3.3.2 By Microorganisms

As we all know, microorganisms are used in the bioremediation of toxic metals by reducing them. In recent years microorganisms have been used for the biosynthesis of nanoparticles by reducing metal ions. Microorganisms have the potential to synthesize nanoparticles as it is cost-effective, eco-friendly, and avoids the use of toxic chemical and energy-intensive procedures. Microorganisms are considered nanofactories as they have a variety of enzymes that have the capability to accumulate and detoxify heavy metals. This enzyme also has the capability of reducing metal salts to produce nanoparticles. Various microorganisms such as yeast, bacteria, and fungi have been discovered to synthesize nanoparticles. Various biochemicals from microorganisms like proteins, cofactors, enzymes, etc. play vital roles in the synthesis of nanoparticles as reducing/capping agents. The mechanism of biosynthesis of nanoparticles by microorganisms involves grabbing target ions from the solution and accumulating the reduced metals in their element form by using enzymes produced by the microorganisms [Table 1]. The mechanism can be classified (according to the place of formation of nanoparticles) into intracellular and extracellular types. In intracellular, the ions are transported into the microorganisms to form nanoparticles in the presence of enzymes. The extracellular involves trapping metal ions on the surface of the cell and reducing it in the presence of enzymes [50]. Many microorganisms can produce inorganic nanoparticles. Various nanoparticles like gold, silver, ZnO, and CdS have been produced via biological methods using microorganisms [51–53].

4 Nanoparticles in Cancer Theranostics

4.1 Nanoparticle-Based Cancer Imaging

Early detection of cancer is necessary for its effective treatment. Different imaging techniques have been employed to precisely detect and locate tumors. Nanoparticles have been utilized for tumor imaging in various modalities such as magnetic resonance imaging (MRI), magnetic particle imaging (MPI), fluorescence imaging/optical imaging, photoacoustic imaging, and positron emission tomography (PET). An overview of some of the imaging methods is summarized in Table 2.

4.1.1 Magnetic Resonance Imaging

The human body contains ^{1}H nuclei, which spin about their axis with no net magnetization due to their random orientation. Under being influenced by a strong magnetic field (B), their spins get aligned along the applied external magnetic field, developing a net magnetic moment (M) while still precising about B. The frequency

Table 2 Overview of commonly used clinical imaging techniques

Imaging method	Advantages	Disadvantages	Nanoparticle contrast agents	References
Magnetic resonance imaging (MRI)	(i) High spatial resolution (10–500 micrometers) (ii) unlimited penetration depth	(i) Low sensitivity to contrast agents (ii) high costs Time intensive	(i) Gadolinium-containing probes (ii) superparamagnetic iron oxide nanoparticles (iii) paramagnetic liposomes and polymers	[129–132]
Magnetic particle imaging (MPI)	(i) Enables the scan to be read with ease. (ii) Relative lost imaging method.	(i) Limited ability to target the tumor and control the exposure. (ii) Limited penetration depth.	(i) Gadolinium nanoparticles. (ii) Iron oxide nanoparticles.	[92, 133, 134]
Computed tomography (CT)	(i) High resolution (20–200 micrometers) (ii) Unlimited penetration depth (iii) Fast (iv) Low costs	(i) Low sensitivity to contrasting agents (ii) insufficient soft tissue contrast without injection of contrast agents	(i) Barium-based nanoparticles (ii) Gold-based nanoparticles (iii) Bismuth nanoparticles	[135–137]
Ultrasound	(i) High temporal and spatial resolution (50–100 micrometers) (ii) Rapidly operable (iii) Real-time imaging (iv) Low costs	Not appropriate for whole-body imaging	(i) Nanobubbles (ii) gas-filled microbubbles	[138–140]
Fluorescence imaging (FI)/ optical imaging	(i) High sensitivity for contrast agents (ii) Low costs	Low penetration depths	(i) Quantum dots (ii) Fluorescent nanoparticle probes	[141, 142]
Photoacoustic imaging (PAI)	(i) High sensitivity (ii) real-time imaging (iii) low costs	(i) Limited penetration depth (ii) relatively low specificity to contrast agents	(i) Gold nanoparticles, gold Nanorods (ii) carbon nanotubes (iii) fluorescent/ dye-loaded nanoparticles	[120, 122, 143–145]

(continued)

Table 2 (continued)

Imaging method	Advantages	Disadvantages	Nanoparticle contrast agents	References
Positron emission tomography (PET)	(i) Unlimited tissue bed penetration. (ii) Used for whole-body imaging. (iii) Detailed anatomical information can be obtained when combined with CT or MRI.	(i) Exposure to radiation. (ii) Low spatial resolution. (iii) Expensive.	(i) Carbon-based nanoparticles. (ii) ^{18}F particles (iii) ^{64}Cu particles.	[146–148]

of precession is quantified by the Larmor equation as $\omega = \gamma B$, where γ the proportionality constant is element-specific. On application of radio wave pulse having a frequency (RF) equal to the precession frequency perpendicular to the direction of B, the ^{1}H nuclei (proton) absorb energy (resonance) and spin out of equilibrium, causing it to flip against the direction of the magnetic field [83]. With the removal of the RF pulse, the phase coherence of the exciting spinning proton ceases to exist. The precessing proton releases energy to attain its equilibrium state through decay in magnetization leading to the proton realigning with B. The energy released during the relaxation process of subsequent echo (gradient or spin echo) of the original RF signal is detected by the receiver coils, which are then processed through computation to obtain the final image. The relaxation process for the proton is of particular interest as it affects the contrast of the image produced during magnetic resonance imaging (MRI). This relaxation process proceeds through two concurrently occurring independent ways:

1. T1 (spin-lattice relaxation).
2. T2 (spin-spin relaxation).

T1 relaxation (or spin-lattice relaxation), in simple terms, is the dissipation of energy of the spins with lattice (or the surrounding environment), which may include neighbouring molecules, spins from other ^{1}H atoms, and solvent molecules [84]. It is the time taken to recover magnetization along the longitudinal axis (parallel to the external magnetic field) to 63% of preexcited net magnetization.

T2 (spin-spin) relaxation is when the transverse component of magnetization has 37% of its exciting level magnetization. It may also be expressed as the time required for the axial spin to return to its resting state. Due to factors such as field inhomogeneity and local field distortions due to molecular interactions (after the removal of the RF pulse), not all nuclei precess have the same frequency (Larmor frequency); instead, there are some minor differences (both positive and negative) in their frequency, which leads to nonuniformity in nuclear dipoles that ultimately leads to the energy being distributed through spin-spin interaction.

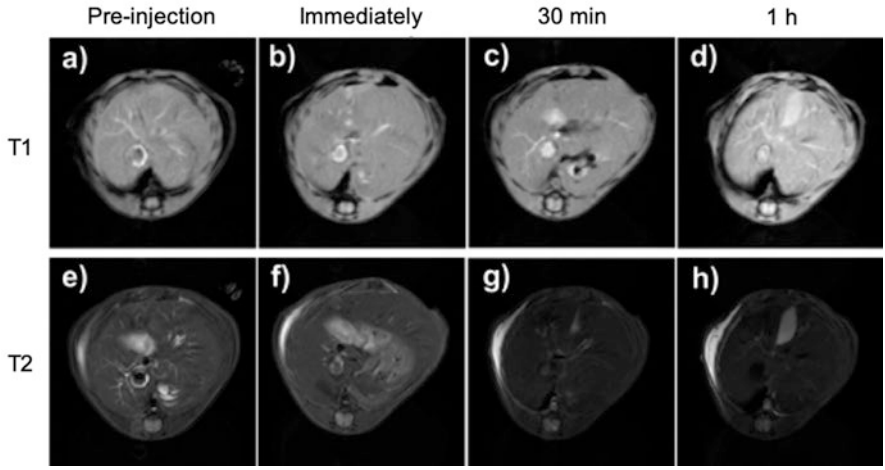

Fig. 2 T1- vs. T2-weighted transverse image of a mice tail vein injected with PEG-stabilized spherical Fe_3O_4/MnO contrast agent [91]. Copyright 2019, American Chemical Society

MRI intensity depends upon local proton density and rate of relaxation; however, the diagnosis that requires better imaging of organs is not possible through intrinsic contrast of MRI (as the signal to noise ratio (SNR) of the images is comparatively low) [85]. Moreover, contrast of the images obtained does not help to identify the stages of the tumor or differentiate between diseased and normal tissues. This is where contrast agents are required due the fact that the local environment affects image quality by exploiting the magnetic behavior of the MNPs. Hence, it is possible to achieve better imaging capabilities by alternating magnetic fields (AMFs) and enhancing the rate of the relaxation process. Further, MRI contrast agents enhance the relaxation process and reduce the relaxation time (T1, T2) for the protons. It is to be noted that though the contrast agents may be labeled as T1 or T2 contrast agents, this nomenclature does not accurately depict its mode of action as T1 agents do impact both T1 and T2 relaxation times. However, their effect on T1 relaxation is greater than on T2 relaxation; likewise, SPIONs (generally considered a T2 contrast agent) impacts T1 relaxation [86].

The characteristic visual difference between the images obtained using T1 and T2 agents is that T1 agents provide positive contrast (bright images), whereas T2 agents result negative contrast in MR images. For example, T1- and T2-weighted transverse images are recorded after injecting PEG-stabilized spherical Fe_3O_4/MnO contrast agent into a BALB/c mice tail vein (Fig. 2). The most extensively utilized T1 agents are Gd^{3+} chelates (e.g., Gd-DTPA) though Mn^{2+} and Fe^{3+} nanoparticles can also be used [87]. Several studies have been reported using ultrasmall superparamagnetic iron oxide nanoparticles as T1 contrast agents [88]. Relaxivity is an important measure to quantify the change in the relaxation time (T1 or T2) that contrast agents can bring to the inherent relaxation times, referred to as longitudinal relaxivity (r1) and transversal relaxivity (r2). The following equation relates the

relaxation time (T) to the concentration of the contrast agent (C), its relaxivity (r), and inherent relaxation time (T0):

$$\frac{1}{T} = \frac{1}{T_0} + r[C]$$

Understanding the factors responsible for impacting relaxation time is instrumental to designing contrast agents that have better sensitivity and significantly that help in selecting the requisite coating materials or conjugates that, besides allowing targeted imaging, aids in enhancing the relaxivity of contrast agents. This interaction between the contrast agents and the surrounding environment is complex. In contrast, the properties of T1 contrast agents (generally paramagnetic cores Gd^{3+}, Mn^{2+}) are impacted by dipole-dipole interaction of core and the H nuclei; for the T2 contrast agent, magnetic inhomogeneity plays the pivotal role, which in turn depends on several factors such as the saturation magnetization of the contrast agent, coating, and the size/radius of MNP [89]. For paramagnetic contrast agents (generally T1), relaxivity also depends on external factors such as temperature and applied magnetic field [90].

4.1.2 Magnetic Particle Imaging

Magnetic particle imaging (MPI) is a tracer imaging modality that can be used to image tissues in vivo based on the spatial distribution of the administered SPIO nanoparticles. A strong magnetic field nonlinearly magnetizes the tracers during imaging against a background of linearly magnetized tissues. In the imaging field of view, SPIONs tracers are saturated by a strong magnetic field gradient, and the unsaturated tracers remain in the vicinity of the field-free region (FFR). On application of an additional time-dependent homogeneous field to the imaging field of view, the particles in the FFR flip induce a signal in the receiver coil. The MPI signal detected is majorly contributed by the tracers at the FFR, allowing MPI spatial encoding [92]. MPI-tailored particles exhibit excellent spatial and temporal resolution, better circulation time, and higher SNR. There is no signal from background tissue in MPI, giving higher contrast. The images obtained using MPI may be used in conjugation with MRI for better diagnosis. SPIONs have been utilized for MPI imaging in vivo, which allows real-time imaging capability. The images obtained had a high spatial resolution, better sensitivity, and specificity [93].

4.1.3 Fluorescence Imaging/Optical Imaging

Optical imaging has been one of the most researched modalities for bioimaging. It allows real-time imaging capabilities. Due to their faster imaging capability, low cost, and non-usage of ionizing radiations, they have been studied as potential

candidates for cancer imaging. Fluorescence imaging quality is mainly dependent on factors such as tissue absorption, scattering, reflection, and autofluorescence [94]. This section will discuss the various types of fluorescence imaging methods that are currently under investigation at different stages of their development and those that are being utilized for in vivo/in vitro imaging applications.

(a) **Up-Conversion and Down-Conversion Nanoparticles.**

The conventional fluorophores suffer from some inherent limitations, such as lower differences in the absorption wavelength and the emission wavelength, making it difficult for the useful signal to be identified; this hinders imaging sensitivity. This causes great difficulty in differentiating the fluorescence signals of the fluorophores. Compared to conventional absorption of multiphoton, the conversion process in up-conversion nanoparticles (UCNPs) and down-conversion nanoparticles (DCNPs) is stepwise, occurring through the real electronic state as adjacent energy levels are very close, so they have better efficiency. These also have better tunability in emission wavelength and can be tuned for the required wavelength to help in imaging deeper tissues [95].

UCNPs are a special class of nanomaterials that can absorb multiple low-energy incident photons (having large wavelength), which causes it to attain an excited state during the transition from the excited state to a stable state; they emit high-energy photons at shorter wavelength, a phenomenon known as the anti-Stokes shift. UCNPs have unique characteristics such as a larger anti-Stokes shift and a larger emission range. These have negligible photobleaching, higher stability, and a longer lifetime [96]. Lanthanide-doped UCNPs have been extensively reported in the literature. It may be composed of a sensitizer part (usually Yb^{3+} is used), an emitter (Tm^{3+}, Ho^{3+} may be used), and a host matrix ($NaYbF_4$, $GdVO_4$, Er^{3+}, Yb^{3+} may be used) [97]. Deep tissue imaging is possible using UCNPs in the NIR range. Cyanine-modified UCNPs have also been reported for use as in vivo molecule monitoring with high sensitivity [98].

On the other hand, DCNP attains an excited state by absorbing high-energy shorter wavelength photons and emitting a long-wavelength photon. Both the conversion processes are nonlinear optical processes. QDs and fluorescent dyes are examples of DCNP. DCNPs have higher quantum yield and SNR. Gold-based nanogapped nanorod DCNP-based fluorescence along with PAI has been used in multimodal imaging to precisely trace drug release and image tumors [99].

(b) **Fluorescence Probe-Based Nanoparticles.**

These nanoparticles may be broadly classified as organic or inorganic molecules. Inorganic molecules mainly are the quantum dots and other fluorescent nanostructures (such as gold nanorods and SWCNTs). The fluorescence probe being used must have the following desirable properties: water solubility, strong fluorescence signal, higher quantum yields, chemical stability in various microenvironment conditions, and high contrast ability [100]. Various types of organic dyes have been studied for use in imaging and image-guided therapy, such as cyanines, methylene blue, squaraine, and porphyrin have been reported [101]. The fluorescence in these dyes is observed as electrons in their molecule transition from the excited state

caused by absorption of incident radiation (UV/visible or infrared range) to a lower energy state during which photons are emitted, leading to fluorescence. Indocyanine green (ICG), an FDA-approved tricarbocyanine dye, has been used to show the efficacy of dyes in tumor imaging [102]. Though dyes such as ICG have been utilized for several decades and have a proven record of their safety, their specificity in imaging cancer is not very encouraging. For example, studies using ICG dye for tumor imaging did allow imaging of the tumors in vivo, but several studies have also pointed out that ICG-based probes nonspecifically accumulate in the liver [103]. This lowers imaging efficiency in such probes. Methylene blue in the NIR has also been utilized to image breast tissue and identify tumors with acceptable sensitivity [104].

Inorganic nanoparticles and nanohybrids have also been researched for application in bioimaging [105]. In the case of metallic nanoparticles, the phenomenon of surface plasmon resonance is observed, which is caused when the light of a certain wavelength is incident on the surface of metallic nanoparticles, causing resonance oscillation of the free conduction electrons imparting it with unique optical properties. The utility of gold nanoparticles (AuNPs) has been studied for passively and actively tumors targeting and their bioimaging in vivo [106, 107]. The excellent chemical stability of AuNPs makes it one of the most suited for bioimaging applications. Novel NIR silica nanoparticle for imaging has also been prepared. It is based on the fluorescence resonance energy transfer principle and has shown to have a significant Stokes shift [108]. Calcium phosphate nanoparticle as an encapsulation of ICG has also been used for in vivo imaging of breast cancer. This has shown to be nontoxic and has better sensitivity to ICG alone [109, 110]. CNTs with surface-modified ligands have also been utilized to image tumors in vivo [111].

Conventionally the fluorescence probes have been irradiated with visible or UV radiation for imaging. However, recently, during the last few decades, studies utilizing the near-infrared (NIR) window for optical imaging applications have been reported and have shown to have significant advantages. Fluorescence in the NIR range has garnered significant interest in optical imaging, the reason being that the radiation's wavelength in range (900–1700 nm) has shown to have minimum absorption by tissues and their constituent organic components, owing to which there is reduced photon scattering and tissue autofluorescence, the background noise is reduced. Imaging properties are significantly enhanced, enabling deeper tissue imaging [112]. Different nanohybrids, QDs, and customized organic dyes have been studied, having peak emission in the NIR range.

(c) **Quantum Dots.**

These are nanocrystalline semiconductors and are engineered to exhibit the required properties. On being exposed to external excitation wavelengths, they emit fluorescence most commonly in the NIR region. The emission of light in quantum dots is due to a phenomenon known as "quantum confinement," which is observed when quantum dots are smaller than their exciton Bohr radius. Compared to organic dyes and other fluorescent probes, QDs have certain advantages such as better, brighter fluorescence emission compared to dyes, better stability, and minimal

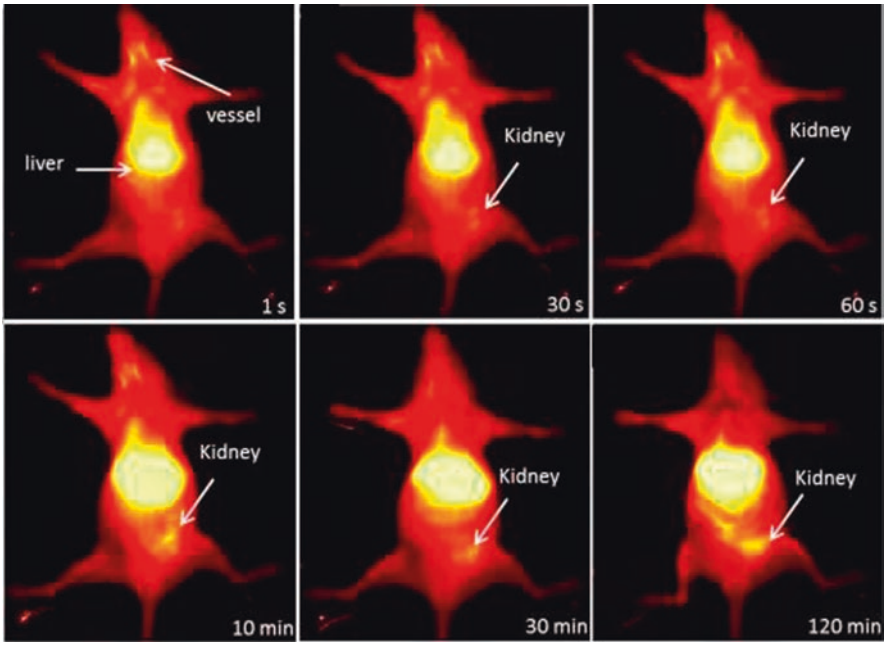

Fig. 3 Fluorescence imaging using graphene quantum dots in mice images at intervals of 1 s, 30 s, 60 s, 10 min, 30 min, and 120 min [119]. Copyright 2019, Elsevier

photobleaching [113]. The fluorescence properties of quantum dots are highly tunable as they depend on their morphology and composition; this provides excellent opportunities in obtaining customized fluorescence based on the specific imaging requirements [114].

The imaging properties of QDs can be further enhanced by improving their efficiency; studies have been conducted using QDs conjugated with antibodies, ligands, and peptides that are sensitive to cancer-related biomarkers. This helps in specifically targeting tumor tissues [115]. CdSe QDs have been extensively studied for in vivo imaging of tumors in mice. While QDs provide excellent imaging and characteristics compared to conventional fluorescence probes such as organic dyes, they have some limitations of their own. Heavy metal-based QDs such as CdSe, when being utilized for imaging, are coated with polymers such as PEG (polyethylene glycol), which makes them quite versatile and nontoxic, but if this external coating is disturbed, then in such scenario, the toxic metallic core may be toxic to cells. The hybrid fluorochrome-QD conjugate may also be used with lower cytotoxicity than Cd [116]. Other metallic QDs such as $AgInS_2$ and ZnS-$AgInS_2$ have lower cytotoxicity and similar imaging capabilities to Cd-based QDs [117]. Graphene quantum dots have also been investigated in bioimaging; they have lower toxicity when compared to Cd-based QDs and have excellent photostability [118]. Fluorescence imaging (FI) using graphene quantum dots dual-doped with both nitrogen and boron in mice images at intervals of 1 s, 30s, 60s, 10 min, 30 min, and 120 min is shown in Fig. 3.

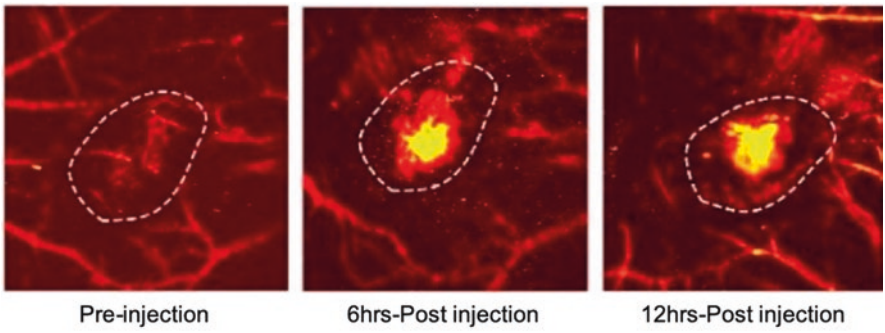

Fig. 4 PAI of tumor in mice 0 h, 6 h, and 12 h after injecting IR783-conjugated chitosan-polypyrrole nanocomposites [126]. Copyright 2021, Springer Nature

4.1.4 Photoacoustic Imaging

Photoacoustic imaging (PAI) is an emerging imaging modality based on converting electromagnetic energy into thermal energy, which generates acoustic pressure waves used to obtain the final image. In this imaging method, tissues that have to be imaged are irradiated with an ultrashort pulsed laser which is absorbed by the tissue, converting light to heat. This results in the generation of an ultrasound wave due to optical absorption and rapid thermal (or thermoelastic) expansion of the tissue. Transducers are used to detect these pressure waves, and an image can be formed based on the contrast due to differences in absorption properties of the tissue components. This hybrid method provides better imaging of deeper tissues while utilizing conventional optical imaging techniques associated with ultrasound [120].

Nanoparticle-based exogenous contrast agents have also been studied in the lab, which has been shown to improve image resolution. AuNPs and SWCNTs are some of the nanomaterials that have already been investigated and have shown promising results [121, 122]. Yamada et al. studied the imaging effectiveness of a conjugate nanoparticle using poly(2-methacryloyloxyethylphosphorylcholine) and 800RS (a hydrophilic, NIR cyanine dye) as a contrast agent in photoacoustic imaging. The 3D images obtained were high quality, better contrast, and high SNR [123]. Gold nanorods coated with silica have also been used for PAI [124]. Methylene blue is also a contrast agent that may be used in PAI, which acts as a hypoxia sensor [125]. Hypoxia is a characteristic of the tumor microenvironment. PA imaging of tumor in mice at 0 hrs, 6 hrs, and 12 hrs after injecting IR783-conjugated chitosan-polypyrrole nanocomposites is determined as shown in Fig. 4.

4.1.5 Positron Emission Tomography (PET)

Positron emission tomography (PET) is a noninvasive, real-time imaging method that utilizes ionizing radiation for bioimaging. It utilizes the nuclear phenomenon of the spontaneous emission of positron emission in radionuclides such as F-18 and carbon-11. Positrons are antimatter to electrons and are similar to electrons, with

the difference being that they carry a positive charge. On being injected into a tissue sample for imaging, the radionuclide undergoes spontaneous decay emitting positron, which encounters an electron in the nearby microenvironment; this leads to the annihilation of the electron and the positron leading to the emission of gamma radiations. The gamma wave detectors receive these gamma radiations, providing signals that are then processed to achieve a detailed image of the tissue sample under consideration [127].

These radionuclides may be doped into nanoparticles which can be made sensitive to the microenvironment and utilize cancer biomarkers to obtain a targeted image of the tumor. PET radiotracers are of different types for imaging tumors as it targets specific cellular events or microenvironments. For example, fluorodeoxyglucose may be utilized to evaluate the cellular glucose metabolism; to evaluate hypoxia microenvironment, 18F-fluoromisonidazole may be used; likewise, to measure cell proliferation, ^{18}F-fluorothymidine may be used [128]. PET provides the ability to evaluate biochemical events in real time with high sensitivity. There is no tissue penetration difficulty and no autofluorescence, but the preparation of the radiotracers is expensive and time-consuming; this makes the PET method unsuitable as a stand-alone method for bioimaging and is therefore generally used after screening is done using cheaper imaging modalities such as MRI, CT, and optical imaging. All the imaging techniques depicted above are shown in Table 2.

4.2 Nanoparticle-Based Cancer Therapy

Nanoparticle-based cancer therapy can be performed by various methods like chemotherapy, magnetic hyperthermia, photothermal therapy, and photodynamic therapy. These different methods of therapy are described in the section below.

4.2.1 Chemotherapy

From the term chemotherapy (CMT) itself, one can decipher that it implies cancer treatment, yet its authentic and historical significance was broader. The term was authored in the early part of the 1900s by Paul Ehrlich [149]. Arsphenamine, the first modern chemotherapeutic agent, used to treat syphilis, is an arsenic compound discovered in the year 1907 [149]. This was subsequently trailed by sulfonamides (sulfa drugs) and penicillin. In today's usage, the sense "any treatment of disease with drugs" is often expressed with the word pharmacotherapy [149]. CMT is an immensely beneficial therapy in the continuous fight against cancer and is regularly utilized related to different medicines. It plays a vital role in bringing down the diseased cells in the body, thereby reducing the probability of spreading cancer and reducing side effect [150]. For instance, in malignant testicular growth, 70% of patients are cured by initial CMT treatment. For patients that experience a recurrence of cancer following CMT treatments, evidence shows that retreating with the

CMT regimen followed by a stem cell transplant is effective on over half of the remaining 30% [150].

From various researches, it is evident that CMT in conjunction with surgery is used in routine to treat colon and rectal cancers [149]. Scientists are creating novel therapeutics with nanomaterials that have novel properties to be utilized in clinical science. Being smaller in size, nanoparticles help to encapsulate drug compounds. The nanoparticles' energy assimilation and reradiation properties permit them to develop further laser and hyperthermia applications, which disturb the diseased tissue [150]. Treatments of cancer are as of now restricted to surgery, radiation, and CMT. Each of the three strategies can harm the tissues, which leads to the incomplete treatment of cancer. Nanotechnology provides the necessary resources to target CMT straightforwardly and specifically to dangerous cells, thereby increasing therapy efficiency [149]. It improves CMT and decreases its unfavorable impacts by directing medications to target malignancy cells specifically. It is highly accurate and, hence, it upgrades the viability of radiotherapies and other current therapy alternatives. Moreover, this has helped to reduce the danger and to upgrade the probabilities for the patients to recover from the disease.

4.2.2 Magnetic Hyperthermia Therapy

MNPs are incredibly fascinating for biomedical applications in the view of their ability to respond to external magnetic fields, which permit their control for targeting in drug delivery. MNPs are very beneficial due to their stable nature in organic conditions and their low toxicity. The MNPs that are widely used in the medical field are mainly made up of iron oxides and ferrites, which are frequently doped with metals like Zn and Ni [151]. Surface coatings/functionalization and encapsulation of the MNPs are carried out to further improve their biocompatibility and bioavailability in targeted drug delivery. Magnetic hyperthermia therapy (MHT) creates the warm environment via a magnetically intervened localized heating of low-recurrence electromagnetic waves through the absorption by MNPs [151]. Thus, if MNPs are delivered inside tumor and the entire patient is exposed to an alternating magnetic field (AMF), the temperature of the tumor will rise. This increase of temperature ideally contracts the size of tumors [151]. MHT is typically applied as an adjuvant to radiotherapy or CMT, to which it fills in as a sensitizer, with an end goal to treat cancer. It utilizes higher temperatures than diathermy and lower temperatures than ablation. Also, when it is combined with radiation treatment, it may be called thermo-radiotherapy.

MHT is a thermal therapy for malignant tumor growth, in view of how MNPs can transform electromagnetic energy into heat by utilizing an AMF at radiofrequency. Many types of research have been explored for MHT-based cancer treatment. MHT was first endeavored in 1957 to treat cancers that had metastasized to the lymph hubs, and it is based upon the standards of limited hyperthermia by utilizing MNPs and consolidating an AMF to generate heat [151]. In MHT, heat is created after neighborhood testimony of MNPs and ensuing utilization of an outer AMF. Generally,

MNPs can produce heat by means of hysteresis losses when exposed to AMFs. The region encased by the hysteresis loop addresses the losses released as heat [152]. The heating capacity relies on the properties of the magnetic material and the AMF boundaries. MHT is widely explored to oppose tumor growth or cancer cell viability by exposure of superparamagnetic nanoparticles to the AMF because of the heat generation via Neel or Brown relaxation mechanism while improving the adequacy of different treatments like radiation and CMT.

For the case of nanostructured magnetic materials, the efficiency of heating hugely relies on a complex relationship between the timescale of the oscillating AMF field vector, magnetic moments, and the intrinsic time-dependent relaxation processes of the nanoparticle. Maier-Hauff et al. effectively showed the decency of superparamagnetic iron oxide nanoparticle-based hyperthermia in human brain growths. They gathered 14 patients with glioblastoma multiforme (GBM), which is a very forceful type of brain cancer. These patients got various medicines consisting of aminosilane-covered superparamagnetic nanoparticles injected straightforwardly into cancer. The nanoparticles were used to raise the temperature in the range of 42–45 °C by exploiting the localized heating by a remotely applied AMF. During the course of the hyperthermia therapy, the patients likewise got fractionated radiation treatment. No critical poison levels were observed [153]. Additionally, Carrouee et al. have created MNPs by combining AgNPs and VNIR color Nile blue (NB) with SPIONs for multimodal imaging dependent on MRI, surface-improved full Raman scattering (SERRS), and NIR-FI [154].

Likewise, Wang et al. have developed MNPs by conjugating fibronectin-focused and endogenous catalyst-activated SPIONs with Cys-Arg-Glu-Lys-Ala (CREKA) peptide and squaraine photosensitizer for MRI-directed FI and PDT of triple-negative breast cancer growths [155]. Very recently, superparamagnetic iron oxide nanoparticles (SPIONs) are widely utilized as highly reliable and efficient MNPs because of their capacity to convey anticancer medications to the cancer site. It helps to instigate magnetic hyperthermia to substitute CMT [18]. In MHT, SPIONs are conveyed (intravenously injected and amassed) at the cancer site, and afterward, the temperature of the growth cells is privately raised to the therapeutic temperature (42–46 °C) on openness to an outer AMF with a radiofrequency [18].

4.2.3 Photodynamic Therapy

Photodynamic therapy (PDT) is a kind of phototherapy involving light and a photosensitizing compound, used in combination with atomic oxygen to evoke cell demise (phototoxicity) [156]. PDT applications mainly include three components: a photosensitizer, a light source, and tissue oxygen [157]. The wavelength of the light source needs to be above the threshold value for exciting the photosensitizer to produce radicals and/or reactive oxygen species. These are free radicals produced through electron abstraction or transfer from a substrate molecule and a highly reactive state of oxygen known as singlet oxygen. Even if one of the components is missing, the desired therapy is not achieved, and the overall efficiency accordingly

requires cautious preparation of both medication and light dosimetry [158]. In general, the medications are given systematically, but since focusing on the process is primarily accomplished through the precise utilization of light, usually, from a laser source, the impact happens to be more localized in action [158]. PDT has a limitation in that it cannot treat advanced diseases because irradiation of the entire body is not possible without the required and adequate number of doses (at least with current technologies). Overall, for cutting-edge diseases, PDT can help improve quality of life and extend survival. PDT can be a specific and remedial therapy for early or localised disease, with numerous expected benefits over available other options.[158].

PDT can be termed as a multistage process: at first, a photosensitizer with negligible dark toxicity is administered, either systemically or topically, without light. Whenever an adequate amount of photosensitizer shows up in the unhealthy/diseased tissue, the photosensitizer is activated by exposure to light for a specified period. The light dose supplies sufficient energy to stimulate the photosensitizer but does not damage neighboring healthy tissue. Target sites are killed by the reactive oxygen [159] and it can be understood that numerous photosensitizers exists for PDT which can be divided into categories that are porphyrins, chlorins, and dyes [160]. Photosensitizers like Allumera, Photofrin, Visudyne, Levulan, Foscan, Metvix, Hexvix, Cysview, and Laserphyrin are commercially available for clinical use, while others being developed, for example, Antrin, Photochlor, Photosens, Photrex, Lumacan, Cevira, Visonac, Amphinex, and Azadipyrromethenes [160–162].

The parts of the cell that photosensitizers target differ significantly. Unlike radiation therapy, where harm is completed by focusing on cell DNA, most photosensitizers target other cell structures. For instance, meta-tetra(hydroxyphenyl)chlorin (mTHPC) restricts the atomic envelope [163], and 5-aminolevulinic acid (ALA) confines in the mitochondria and methylene blue in the lysosomes [164, 165]. PDT is well-known for its use in the treatment of skin inflammation. It is used in clinical settings to treat a wide range of conditions, including wet age-related macular degeneration, psoriasis, and atherosclerosis, and has shown some efficacy in viral medicines, including herpes. It likewise treats threatening cancers including head and neck, lung, bladder, and specific skin [157]. The innovation has also been tried to treat prostate malignancy in a canine model and in human prostate disease patients [166, 167]. It is perceived as a treatment system that is both negligibly intrusive and insignificantly harmful. Other light-based and laser treatments, for example, laser wound recuperating and revival or great beat light hair expulsion, do not need a photosensitizer [159]. Photosensitizers have been used to sanitize blood plasma and water to eliminate blood-borne infections and have been considered for rural utilizations, including herbicides and insecticides. Photodynamic treatment's benefits decrease the requirement for a sensitive medical procedure, extensive recovery, and negligible scar tissue arrangement and distortion. An incidental effect is the related photosensitization of skin tissue [159].

4.2.4 Photothermal Therapy

Photothermal therapy (PTT) refers to using electromagnetic radiation (in infrared frequencies) to treat different ailments, including cancers. This methodology is an expansion of PDT, in which a photosensitizer is energized using a particular band light. The heat released during the activation of the sensitizer to the exciting stage helps to kill the cancer cells. Photodynamic treatment does not harm the surrounding cells because the photosensitizers will generally develop in unusual cells, and the light is centered straight to them, thus not impacting the other cells of the body. Photodynamic treatment does not cause scars, which is helpful for individuals with skin malignancies and precancers. Dissimilar to PDT, PTT does not require the interaction of oxygen with cancer cells. Current investigations additionally show that PTT can utilize longer-frequency light, which is less energetic and, in this way, less damaging to different cells and tissues. Treatment of solid tumors can be efficiently done using such kind of treatment. The current research mainly focuses on nanomaterials for the PTT due to their size and efficacy over other sized particles. The permeability and retention effect are usually high in nanoscale, making it a strong contender for PTT. It has been observed that whenever a tumor is developed, blood vessels are required to improve its growth; these blood vessels located nearer to the tumor have different properties compared to the regular blood vessels. These developments can be prevented by using nanoparticles like gold nanorods (AuNRs), gold nanoshells, etc.

The practicality of utilizing gold nanorods was observed for both cancer cell imaging and photothermal therapy [168]. The authors conjugated antibodies (anti-EGFR monoclonal antibodies) to the outer layer of gold nanorods, permitting the gold nanorods to tie explicitly to certain threatening malignant growth cells (HSC and HOC dangerous cells). After brooding the cells with the gold nanorods, an 800 nm Ti-sapphire laser was utilized to light the cells at different forces. The creators revealed that successful annihilation of the threatening malignant growth cells was observed while nonmalignant cells were safe. When AuNRs are presented to NIR light, the oscillating magnetic field of light makes the free electrons oscillate collectively [169]. It was also experimentally observed that altering the shape and size of AuNRs correspondingly changes the assimilated wavelength. An ideal frequency would be between 700 and 1000 nm because natural tissue is optically transparent at these wavelengths [170]. While all gold nanoparticles (AuNP) are delicate to change in their shape and size, the properties of Au nanorods are susceptible to any adjustment of any of their measurements regarding their length and width or their perspective proportion. At the point when light gleams on a metal nanoparticle, the nanoparticle develops a dipole swaying along with the heading of the electric field. When the oscillation arrives at its maximum value, the corresponding frequency is known as the surface plasmon resonance (SPR) [169]. There are two SPR spectrum bands in AuNRs: one in the NIR region caused by its longitudinal oscillation (with a longer wavelength, it tends to become stronger) and one in the visible region caused by the transverse electronic oscillation (at shorter wavelengths, it becomes weak) [171]. An increase in light absorption for the particle is

characterized by the SPR [169]. It was noticed that the electrons energized by the NIR lose energy very rapidly after absorption due to the collisions between electrons. Whenever the relaxation of the electrons occurs, the energy is released, which is called a phonon that then heats the environment. This heating of the AuNP will help to eliminate the cancerous cells. This interaction is seen when a laser has a constant wave onto the AuNP [169].

Gold nanoshells, are silica nanoparticles that have been coated with a thin layer of gold. PEG linkers were used to associate them to antibodies (anti-HER2 or anti-IgG) [172]. After incubating SKBr3 cancer cells with the gold nanoshells, the cells were irradiated with an 820 nm laser. Then, it was observed that only the cells incubated with gold nanoshells conjugated with the specific antibody were damaged by the laser (anti-HER2). Another type of gold nanoshell is developed on liposomes that act as a soft template to encapsulate drugs inside and/or in a bilayer which is studied for triggered drug release by laser light [173]. PTT alone can wipe out the cancer cells in essential cancer or local lymphatic metastasis in the shallow tissues to reduce their further metastasis in distant organs [174]. However, due to the inhomogeneous distribution of heat within these tissues, PTT alone is insufficient to destroy disease cells and prevent cancer recurrence and metastasis (formation of secondary cancer cells located at a certain distance from a primary site of cancer).

5 Multimodal Theranostics

The various imaging and therapy techniques each have their own set of limitations. It is pretty evident that methods that can provide the combined effect of different imaging and therapeutic modalities which could significantly enhance therapeutic/imaging efficacy for effective cancer theranostics. Multifunctional nanoparticles have been investigated for multimodal treatment and have shown promising results. This section discusses the different multimodal techniques currently under investigation catering to combined imaging and therapy.

5.1 Multimodal Imaging

Cancer detection is highly complex. The survivability of cancer patients depends significantly on its early diagnosis and treatment. The different methods that have been developed for cancer detection are still not perfect, and each of the imaging methods has some of its own shortcomings and advantages. The multimodal imaging method involves utilizing more than one of the bioimaging methods in conjugation. This method helps to negate the shortcomings of the particular imaging methods, thereby providing combined imaging modality having essential imaging features such as real-time imaging capability, high sensitivity, better contrast resolution, and enhanced imaging with high SNR.

Different strategies are being investigated to achieve multimodal imaging. For example, fluorescence/MRI imaging can be used together for molecular imaging. While fluorescence imaging has high sensitivity and planar resolution, it has limitations such as low spatial resolution and lower penetration capability. Utilizing MRI can improve upon the limitations of fluorescence imaging as MRI has better penetration capability and spatial resolution. Gd-doped UCNPs can also be utilized for such types of multimodal imaging [175]. Dual-modal imaging by MRI/PET using radiolabeled SPIO nanoparticles has also been studied, and the resulting image provided excellent resolution [176]. Gd_2O_3:Eu^{3+} nanorods have been studied as a bifunctional nanoparticle with magnetic and luminescence properties enabling high

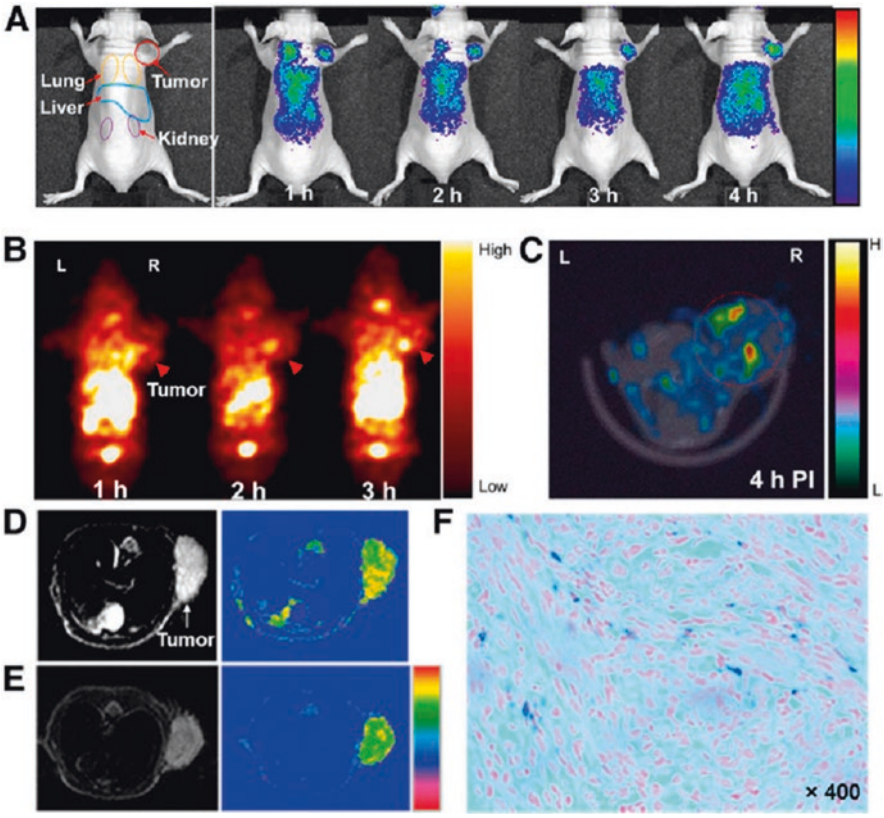

Fig. 5 Representation of multimodality tumor imaging using cMBP-GA-ATP@SPIONs. (**a**) In vivo noninvasive near-infrared fluorescent images of mice with U87MG tumors were taken at 1, 2, 3, and 4 h after injection of CMG-ATP@SPIONs. (**b**) In vivo, static planar g images of mice with U87MG tumors were taken at 1, 2, and 3 h after injection of 125I-cMBP-GA-ATP@SPIONs. (**c**) Transverse SPECT/CT image of the same mouse for 4 hours after injection. In vivo, T2-weighted MR images of mice with U87MG tumors were obtained before (**d**) and at 3 hours after (**e**) injection of cMBP-GA-ATP@SPIONs. (**f**) Staining was done using Prussian blue on tumor sections [182]. Copyright 2013, Society of Nuclear Medicine

contrast cell imaging and low autofluorescence [177]. Fluorescence/PET dual-modal imaging has also been successful in imaging triple-negative breast cancer [178]. Similarly, different combinations such as fluorescence/CT, PAI/MRI, and many other combinations of the different imaging modalities present are also possible to have trimodal imaging combining fluorescence/MRI/CT.

Other strategies such as developing contrast agents that allow multimodal T1-T2 imaging or developing nanocomposites that exhibit diverse properties, say fluorescence and magnetism, are also being investigated. Silica-coated Fe_2O_3 has been reported to exhibit fluorescence besides having magnetic nature [179]. MNP-QD conjugates as imaging nanoprobes have also been reported [180]. Nanoparticles conjugated with fluorescent polymer have been successfully prepared. PET/optical multimodal imaging has been studied using hyperbranched polymers labeled with organic dye and ^{64}Cu, the former is responsible for optical properties, and the latter is responsible for radioactivity that enables PET imaging [181]. Multimodal imaging can solve the limitations to the individual imaging modalities and may serve as a prime tool in detecting cancer in its initial stages for effective treatment. Multimodal imaging based on fluorescence, SPEC/CT, and MRI investigated using the mice model is shown in Fig. 5.

5.2 Multimodal Therapy

As the name suggests, multimodal therapy (MMT) combines two or more therapy to overcome the limitation of monotherapy. By combining various sorts of therapy together, MMTs can enhance cancer therapy. Various multimodal theranostics studies have been performed using different multifunctional nanoparticles combining therapeutic and imaging approaches. Ge et al. have illustrated the image-directed simultaneous PDT/PTT therapeutics and fluorescence imaging through biocompatible and photograph stable CD-based theranostic agents (evident from Fig. 6) [183]. In this work, CDs with various sizes (610 nm) are formulated by utilizing polythiophene benzoic acid (Fig. 6a, b), from which red light was observed on excitation. CDs generated singlet oxygen species and heat all the while under laser illumination (Fig. 6c) showed promising in vitro and in vivo results in the single/combined PDT and PTT cancer therapy as shown in Figure 6 (Fig. 6d, e).

Dai et al. formulated dendrimer-like MSN with hierarchical pores (HPSNs) as pH-responsive MNPs, which can be used in vivo targeted cancer imaging and therapy [184]. Moreover, Sun et al. have prepared DOX-conjugated, Gd-doped, ICG-loaded, and thermosensitive liposome-based MSNs as (MNPs) [185], which have demonstrated outstanding potential in cancer treatment via multimodal imaging (via NIR fluorescence imaging, PAI, and MRI) and also synergetic therapies (via PDT, PTT, and CMT). Recently, Yang et al. have developed perylene diimide-hybridized and ^{64}Cu-chelated photo-theranostic MSNs [186], which displayed a better PET imaging functionality with improved fluorescence and photoacoustic imaging capabilities.

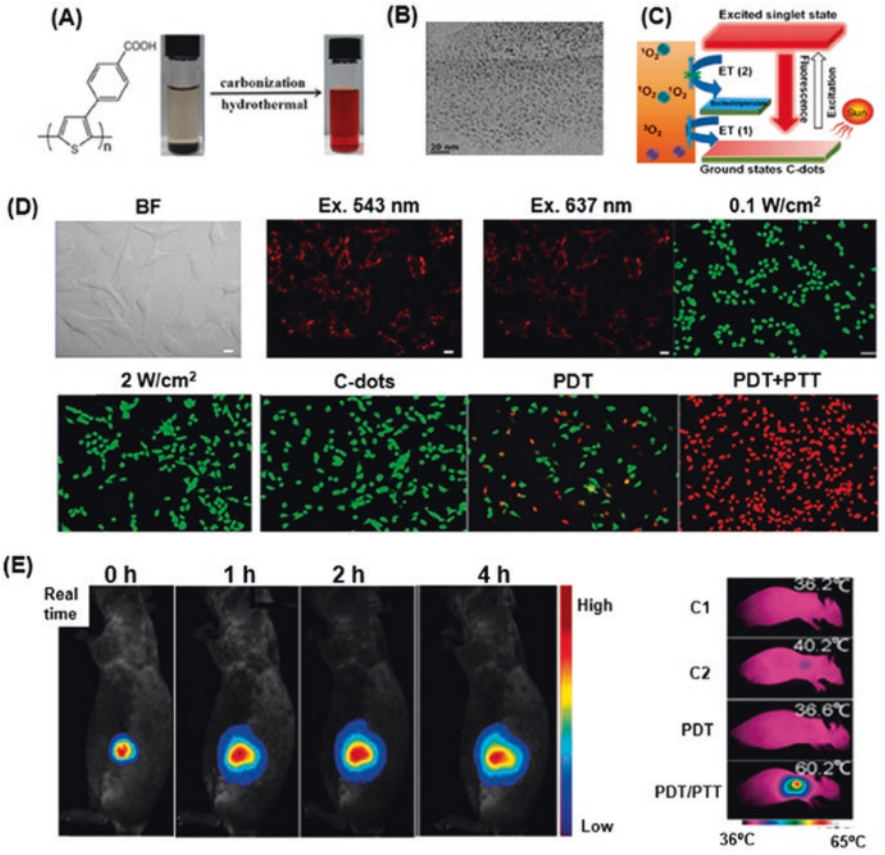

Fig. 6 PDT/PTT combined with C-dot-based bioimaging. (**a**) Fabrication of C-dots. (**b**) TEM image of C-dots. (**c**) The mechanism for the single oxygen $^1O_2$ generation by C-dots. (**d**) In vitro imaging and PDT/PTT with cancer cells. (**e**) Fluorescence images of calcein-AM/PI-stained cancer cells with laser irradiation [18]. Copyright 2021, Elsevier

Considering the results of different studies, it has been observed that multimodal therapy has the best endurance and efficacy compared to other monotherapies. However, further investigations are required to examine and refine the best accessible treatments for the different tumor types using the various possible multimodal treatment modalities.

6 Conclusion and Future Prospects

The biomedical use of nanotechnology is alluded to as nanomedicine, and this is made conceivable by a vast scope of scientific approaches and the advent of clinical techniques. One such methodology is the utilization of nanoparticles in

theranostics. A definitive point for consolidating nanomedicine and theranostics is to improve tumor diagnosis techniques and achieve patient-explicit treatment results. This can be achieved due to their high potential to target explicit organs or tissues. Just as their ability to be controlled with multifunctionality, theranostic nanoparticles have critical benefits that are splendidly appropriate for early cancer diagnosis and targeted therapy. In tumor therapy, nanotechnology can play a pivotal role in bettering conventional CMT besides being useful in other therapies such as MHT, PDT, and PTT. Moreover, different bioimaging modalities which are currently under development utilizing nanoprobes have shown promising results. The advantage of nanoprobes is that they can precisely track molecular activities occurring at the cellular level providing significant insights into the cellular mechanisms. This can be highly beneficial in cancer treatment, where early detection of malignancy directly impacts patient survivability. Furthermore, by introducing explicit modifications on the nanoparticle surfaces, designated controllable medication discharge and atomic imaging identification have been accomplished. Moreover, nanomaterials conjugated with antibodies and peptides have been shown to provide powerful focusing capacities to theranostic nanoparticles [187].

Considering the aspect of multifunctional nanomaterials synthesis, it is necessary to have a repeatable, scalable, and practical assembling strategy to synthesize theranostic nanoparticles. With the current synthesis techniques, it is pretty challenging to have a cost-effective solution for large-scale nanoparticle synthesis which can be used for medical applications. It is also essential to understand the basic pharmacokinetics of the nanoprobes being used to enhance their efficiency and also to reduce their developmental time. The potential toxicity of nanoparticles is also a significant impediment to their in vivo application. Another possible issue regarding the commercial success of nano-based theranostics is the expense of new medication advancements. Contrasted to the continued utilization of existing findings and treatment strategies, new medication improvements require a great deal of labor, material assets, and time. It merits pondering how to persuade manufacturers to put resources into the innovative work of theranostic nanoparticles.

To conclude, nanotechnology can effectively change how conventionally tumors are diagnosed and treated. It may be the necessary tool required for effective cancer treatment through efficient/combined diagnosis, therapy, and monitoring. Multimodal theranostics using multifunctional nanoparticles could be the way forward, given their effectiveness and customizability in cancer treatment, but further investigation on their biocompatibility and bioavailability is necessary.

Acknowledgments Dipak Maity would like to thank the University of Petroleum and Energy Studies (UPES) for getting in-house financial support (SEED Funding: UPES/R&D-HS/2402 2022/08) and all other support. Satya Ranjan Sahoo would like to thank the University Grants Commission of India (UGC) for providing a Junior Research Fellowship (NTA reference number—191620074817). Sumit Saha wishes to thank Prof. Suddhasatwa Basu, Director, CSIR-Institute of Minerals & Materials Technology, Bhubaneswar, India, for in-house financial support (Grant number: CSIR-IMMT-OLP-112) and requisite permissions.

References

1. Ferlay J, Colombet M, Soerjomataram I, Mathers C, Parkin D, Piñeros M, Znaor A, Bray F. Estimating the global cancer incidence and mortality in 2018: GLOBOCAN sources and methods. Int J Cancer. 2019;144(8):1941–53.
2. Raja IS, Kang MS, Kim KS, Jung YJ, Han D-W. Two-dimensional theranostic nanomaterials in cancer treatment: state of the art and perspectives. Cancers. 2020;12(6):1657.
3. Fan Z, Fu PP, Yu H, Ray PC. Theranostic nanomedicine for cancer detection and treatment. Journal of food drug analysis. 2014;22(1):3–17.
4. Jin C, Wang K, Oppong-Gyebi A, Hu J. Application of nanotechnology in cancer diagnosis and therapy – a mini-review. Int J Med Sci. 2020;17(18):2964.
5. Jokerst JV, Gambhir SS. Molecular imaging with theranostic nanoparticles. Acc Chem Res. 2011;44(10):1050–60.
6. Chen F, Ehlerding EB, Cai W. Theranostic nanoparticles. J Nucl Med. 2014;55(12):1919.
7. Wu K, Su D, Liu J, Saha R, Wang J-P. Magnetic nanoparticles in nanomedicine: a review of recent advances. Nanotechnology. 2019;30(50):502003.
8. Akbarzadeh A, Samiei M, Davaran S. Magnetic nanoparticles: preparation, physical properties, and applications in biomedicine. Nanoscale Res Lett. 2012;7(1):144.
9. Maity D, Kandasamy G, Sudame A. Superparamagnetic iron oxide nanoparticles for cancer theranostic applications. In: Rai M, Jamil B, editors. Nanotheranostics: applications and limitations. Cham: Springer; 2019. p. 245–76.
10. Patel KD, Singh RK, Kim H-W. Carbon-based nanomaterials as an emerging platform for theranostics. Materials Horizons. 2019;6(3):434–69.
11. Testa C, Zammataro A, Pappalardo A, Trusso Sfrazzetto G. Catalysis with carbon nanoparticles. RSC Adv. 2019;9(47):27659–64.
12. Kramer SA, Lin W. Silica-based nanoparticles for biomedical imaging and drug delivery applications. In: Handbook of nanobiomedical research. Singapore, World Scientific. p. 403–37.
13. Bitar A, Ahmad NM, Fessi H, Elaissari A. Silica-based nanoparticles for biomedical applications. Drug Discov Today. 2012;17(19):1147–54.
14. Yang Y, Zhang M, Song H, Yu C. Silica-based nanoparticles for biomedical applications: from nanocarriers to biomodulators. Acc Chem Res. 2020;53(8):1545–56.
15. Selvarajan V, Obuobi S, Ee PLR. Silica nanoparticles – a versatile tool for the treatment of bacterial infections. Front Chem. 2020;8(602)
16. Couleaud P, Morosini V, Frochot C, Richeter S, Raehm L, Durand J-O. Silica-based nanoparticles for photodynamic therapy applications. Nanoscale. 2010;2(7):1083–95.
17. Kumar HK, Venkatesh N, Bhowmik H, Kuila A. Metallic nanoparticle: a review, Biomed J Scientific/Tech Res. 2018;4(2):3765–75.
18. Kandasamy G, Maity D. Multifunctional theranostic nanoparticles for biomedical cancer treatments – a comprehensive review. Mater Sci Eng C. 2021;127:112199.
19. Gomes HIO, Martins CSM, Prior JAV. Silver nanoparticles as carriers of anticancer drugs for efficient target treatment of cancer cells. Nanomaterials. 2021;11(4):964.
20. Jain S, Hirst DG, O'Sullivan JM. Gold nanoparticles as novel agents for cancer therapy. Br J Radiol. 2012;85(1010):101–13.
21. Rao JP, Geckeler KE. Polymer nanoparticles: preparation techniques and size-control parameters. Prog Polym Sci. 2011;36(7):887–913.
22. Lu X-Y, Wu D-C, Li Z-J, Chen G-Q. Polymer nanoparticles (Chpater 7). In: Villaverde A, editor. Progress in molecular biology and translational science, vol. 104. Cambridge: Academic; 2011. p. 299–323.
23. Zielińska A, Carreiró F, Oliveira AM, Neves A, Pires B, Venkatesh DN, Durazzo A, Lucarini M, Eder P, Silva AM, Santini A, Souto EB. Polymeric nanoparticles: production, characterization. Toxicol Ecotoxicol. 2020;25(16):3731.

24. García-Pinel B, Porras-Alcalá C, Ortega-Rodríguez A, Sarabia F, Prados J, Melguizo C, López-Romero JM. Lipid-based nanoparticles: application and recent advances in cancer treatment. Nanomaterials. 2019;9(4):638.
25. Mittal P, Saharan A, Verma R, Altalbawy FMA, Alfaidi MA, Batiha GE-S, Akter W, Gautam RK, Uddin MS, Rahman MS. Dendrimers: a new race of pharmaceutical Nanocarriers. Biomed Res Int. 2021;2021:8844030.
26. Abbasi E, Aval SF, Akbarzadeh A, Milani M, Nasrabadi HT, Joo SW, Hanifehpour Y, Nejati-Koshki K, Pashaei-Asl R. Dendrimers: synthesis, applications, and properties. Nanoscale Res Lett. 2014;9(1):247.
27. Amendola V, Meneghetti M. Laser ablation synthesis in solution and size manipulation of noble metal nanoparticles. Phys Chem Chem Phys. 2009;11(20):3805–21.
28. Pimpin A, Srituravanich W. Review on micro-and nanolithography techniques and their applications. Eng J. 2012;16(1):37–56.
29. Hulteen JC, Treichel DA, Smith MT, Duval ML, Jensen TR, Van Duyne RP. Nanosphere lithography: size-tunable silver nanoparticle and surface cluster arrays. J Phys Chem B. 1999;103(19):3854–63.
30. Altissimo M. E-beam lithography for micro-/nanofabrication. Biomicrofluidics. 2010;4(2):026503.
31. Corbierre MK, Beerens J, Lennox RB. Gold nanoparticles generated by electron beam lithography of Gold(I)−thiolate thin films. Chem Mater. 2005;17(23):5774–9.
32. Yadav TP, Yadav RM, Singh DP. Mechanical milling: a top down approach for the synthesis of nanomaterials and nanocomposites. Nanosci Nanotechnol. 2012;2(3):22–48.
33. Rane AV, Kanny K, Abitha VK, Thomas S. Methods for synthesis of nanoparticles and fabrication of nanocomposites (Chapter 5). In: Mohan Bhagyaraj S, Oluwafemi OS, Kalarikkal N, Thomas S, editors. Synthesis of inorganic nanomaterials. Woodhead Publishing; 2018. p. 121–39.
34. Kolahalam LA, Kasi Viswanath IV, Diwakar BS, Govindh B, Reddy V, Murthy YLN. Review on nanomaterials: synthesis and applications. Mater Today Proc. 2019;18:2182–90.
35. Carlsson J-O, Martin PM. Chemical vapor deposition (Chapter 7). In: Martin PM, editor. Handbook of deposition technologies for films and coatings. 3rd ed. Boston: William Andrew Publishing; 2010. p. 314–63.
36. Sun L, Yuan G, Gao L, Yang J, Chhowalla M, Gharahcheshmeh MH, Gleason KK, Choi YS, Hong BH, Liu Z. Chemical vapour deposition. Nature Rev Methods Primers. 2021;1(1):5.
37. Hoar TP, Schulman JH. Transparent water-in-oil dispersions: the Oleopathic hydro-micelle. Nature. 1943;152(3847):102–3.
38. Ganguli AK, Ganguly A, Vaidya S. Microemulsion-based synthesis of nanocrystalline materials. Chem Soc Rev. 2010;39(2):474–85.
39. Djurisic AB, Xi YY, Hsu YF, Chan WK. Hydrothermal synthesis of nanostructures. Recent Pat Nanotechnol. 2007;1(2):121–8.
40. Yang G, Park S-J. Conventional and microwave hydrothermal synthesis and application of functional materials: a review. Materials. 2019; 12(7).
41. Odularu A T. Metal nanoparticles: thermal decomposition, biomedicinal applications to cancer treatment, and future perspectives. Bioinorg Chem Appl. 2018;2018:9354708.
42. Thakkar KN, Mhatre SS, Parikh RY. Biological synthesis of metallic nanoparticles. Nanomedicine. 2010;6(2):257–62.
43. Soni V, Raizada P, Singh P, Cuong H N, S R, Saini A, Saini R V, Le Q V, Nadda A K, Le T-T, Nguyen V-H. Sustainable and green trends in using plant extracts for the synthesis of biogenic metal nanoparticles toward environmental and pharmaceutical advances: a review. Environ Res. 2021; 202: 111622.
44. Iravani S. Green synthesis of metal nanoparticles using plants. Green Chem. 2011;13(10):2638–50.
45. Mittal AK, Chisti Y, Banerjee UC. Synthesis of metallic nanoparticles using plant extracts. Biotechnol Adv. 2013;31(2):346–56.

46. Chandran SP, Chaudhary M, Pasricha R, Ahmad A, Sastry M. Synthesis of gold nanotriangles and silver nanoparticles using Aloevera plant extract. Biotechnol Prog. 2006;22(2):577–83.
47. Song JY, Kim BS. Rapid biological synthesis of silver nanoparticles using plant leaf extracts. Bioprocess Biosyst Eng. 2008;32(1):79.
48. Ahmed S, Ahmad M, Swami BL, Ikram S. A review on plants extract mediated synthesis of silver nanoparticles for antimicrobial applications: a green expertise. J Adv Res. 2016;7(1):17–28.
49. Jadoun S, Arif R, Jangid NK, Meena RK. Green synthesis of nanoparticles using plant extracts: a review. Environ Chem Lett. 2021;19(1):355–74.
50. Zhang X, Yan S, Tyagi RD, Surampalli RY. Synthesis of nanoparticles by microorganisms and their application in enhancing microbiological reaction rates. Chemosphere. 2011;82(4):489–94.
51. Li X, Xu H, Chen Z-S, Chen G. Biosynthesis of nanoparticles by microorganisms and their applications. 2011; 2011: Article 8.
52. Narayanan KB, Sakthivel N. Biological synthesis of metal nanoparticles by microbes. Adv Colloid Interf Sci. 2010;156(1):1–13.
53. Hulkoti NI, Taranath TC. Biosynthesis of nanoparticles using microbes – a review. Colloids Surf B: Biointerfaces. 2014;121:474–83.
54. Avasthi A, Caro C, Pozo-Torres E, Leal M P, García-Martín M L. Magnetic nanoparticles as MRI contrast agents. Surface-Mod Nanobiomater Electrochem Biomed Appl. 2020; 49–91.
55. Paysen H, Loewa N, Stach A, Wells J, Kosch O, Twamley S, Makowski M R, Schaeffter T, Ludwig A, Wiekhorst F. 3D-imaging and quantification of magnetic nanoparticle uptake by living cells. arXiv preprint arXiv:.01259. 2019.
56. Kratz H, Taupitz M, Ariza de Schellenberger A, Kosch O, Eberbeck D, Wagner S, Trahms L, Hamm B, Schnorr J. Novel magnetic multicore nanoparticles designed for MPI and other biomedical applications: from synthesis to first in vivo studies. PloS One. 2018;13(1):e0190214.
57. Giustini A J, Petryk A A, Cassim S M, Tate J A, Baker I, Hoopes P J. Magnetic nanoparticle hyperthermia in cancer treatment. Nano Life. 2010; 1(01n02): 17–32.
58. Jose J, Kumar R, Harilal S, Mathew GE, Parambi DGT, Prabhu A, Uddin M, Aleya L, Kim H, Mathew B. Magnetic nanoparticles for hyperthermia in cancer treatment: an emerging tool. Environ Sci Pollut Res. 2020;27(16):19214–25.
59. Kudr J, Haddad Y, Richtera L, Heger Z, Cernak M, Adam V, Zitka O. Magnetic nanoparticles: from design and synthesis to real world applications. Nano. 2017;7(9):243.
60. Sundaram P, Abrahamse H. Phototherapy combined with carbon nanomaterials (1D and 2D) and their applications in cancer therapy. Materials. 2020;13(21):4830.
61. Casais-Molina M, Cab C, Canto G, Medina J, Tapia A. Carbon nanomaterials for breast cancer treatment. J Nanomater. 2018;2018
62. Shibu ES, Hamada M, Murase N, Biju V. Nanomaterials formulations for photothermal and photodynamic therapy of cancer. J Photochem Photobiol C Photochem Rev. 2013;15:53–72.
63. Rao N, Singh R, Bashambu L. Carbon-based nanomaterials: synthesis and prospective applications. Materials Today: Proceedings. 2021;44:608–14.
64. Ganash EA, Al-Jabarti GA, Altuwirqi RM. The synthesis of carbon-based nanomaterials by pulsed laser ablation in water. Mater Res Express. 2019;7(1):015002.
65. Sajjadi M, Nasrollahzadeh M, Jaleh B, Soufi GJ, Iravani S. Carbon-based nanomaterials for targeted cancer nanotherapy: recent trends and future prospects. J Drug Target. 2021;29(7):716–41.
66. Zheng Z, Jia Z, Qu C, Dai R, Qin Y, Rong S, Liu Y, Cheng Z, Zhang R. Biodegradable silica-based Nanotheranostics for precise MRI/NIR-II fluorescence imaging and self-reinforcing antitumor therapy. Small. 2021;17(10):2006508.
67. Li D, Liu Y, Yu S, Zhang D, Wang X, Zhong H, He K, Wang Y, Wu Y-X. A two-photon fluorescence silica nanoparticle-based FRET nanoprobe platform for effective ratiometric bioimaging of intracellular endogenous adenosine triphosphate. Analyst. 2021;146(15):4945–53.

68. Chen M, Hu J, Wang L, Li Y, Zhu C, Chen C, Shi M, Ju Z, Cao X, Zhang Z. Targeted and redox-responsive drug delivery systems based on carbonic anhydrase IX-decorated mesoporous silica nanoparticles for cancer therapy. Sci Rep. 2020;10(1):1–12.
69. Finnie KS, Bartlett JR, Barbé CJ, Kong L. Formation of silica nanoparticles in microemulsions. Langmuir. 2007;23(6):3017–24.
70. Zhou Y, Quan G, Wu Q, Zhang X, Niu B, Wu B, Huang Y, Pan X, Wu C. Mesoporous silica nanoparticles for drug and gene delivery. Acta Pharm Sin B. 2018;8(2):165–77.
71. Mao K, Zhang W, Yu L, Yu Y, Liu H, Zhang X. Transferrin-decorated protein-lipid hybrid nanoparticle efficiently delivers cisplatin and docetaxel for targeted lung cancer treatment. Drug Design Develop Therapy. 2021;15:3475.
72. Kalaycioglu GD, Aydogan N. Preparation and investigation of solid lipid nanoparticles for drug delivery. Colloids Surf A Physicochem Eng Aspects. 2016;510:77–86.
73. García-Pinel B, Porras-Alcalá C, Ortega-Rodríguez A, Sarabia F, Prados J, Melguizo C, López-Romero JM. Lipid-based nanoparticles: application and recent advances in cancer treatment. Nano. 2019;9(4):638.
74. C-g Q, Y-l C, P-j F, X-z X, Dong M, Yu J-c, Hu Q-y, Shen Q-d GZ. Conjugated polymer nanomaterials for theranostics. Acta Pharmacol Sin. 2017;38(6):764–81.
75. Zielińska A, Carreiró F, Oliveira AM, Neves A, Pires B, Venkatesh DN, Durazzo A, Lucarini M, Eder P, Silva AM. Polymeric nanoparticles: production, characterization, toxicology and ecotoxicology. Molecules. 2020;25(16):3731.
76. Palanikumar L, Al-Hosani S, Kalmouni M, Nguyen VP, Ali L, Pasricha R, Barrera FN, Magzoub M. pH-responsive high stability polymeric nanoparticles for targeted delivery of anticancer therapeutics. Commun Biol. 2020;3(1):1–17.
77. Wong KH, Lu A, Chen X, Yang Z. Natural ingredient-based polymeric nanoparticles for cancer treatment. Molecules. 2020;25(16):3620.
78. Sztandera K, Gorzkiewicz M, Klajnert-Maculewicz B. Gold nanoparticles in cancer treatment. Mol Pharm. 2018;16(1):1–23.
79. Yu Z, Gao L, Chen K, Zhang W, Zhang Q, Li Q, Hu K. Nanoparticles: a new approach to upgrade cancer diagnosis and treatment. Nanoscale Res Lett. 2021;16(1):1–17.
80. Marinescu L, Ficai D, Oprea O, Marin A, Ficai A, Andronescu E, Holban A-M. Optimized synthesis approaches of metal nanoparticles with antimicrobial applications. J Nanomater. 2020;2020
81. Jamkhande PG, Ghule NW, Bamer AH, Kalaskar MG. Metal nanoparticles synthesis: an overview on methods of preparation, advantages and disadvantages, and applications. J Drug Deliv Sci Technol Cancer Res Treat. 2019;53:101174.
82. Sharma A, Goyal AK, Rath G. Recent advances in metal nanoparticles in cancer therapy. J Drug Target. 2018;26(8):617–32.
83. Grover VP, Tognarelli JM, Crossey MM, Cox IJ, Taylor-Robinson SD, McPhail MJ. Magnetic resonance imaging: principles and techniques: lessons for clinicians. J Clin Experim Hepatol. 2015;5(3):246–55.
84. Issa B, Obaidat IM. Magnetic nanoparticles as MRI contrast agents. Magn Reson Imaging. 2019;378:40.
85. Alvares RD, Szulc DA, Cheng H-L. A scale to measure MRI contrast agent sensitivity. Sci Rep. 2017;7(1):1–9.
86. Liu Z, Cai J, Su H, Yang J, Sun W, Ma Y, Liu S, Zhang C. Feasibility of USPIOs for T 1-weighted MR molecular imaging of tumor receptors. RSC Adv. 2017;7(50):31671–81.
87. Huang G, Li H, Chen J, Zhao Z, Yang L, Chi X, Chen Z, Wang X, Gao J. Tunable T 1 and T 2 contrast abilities of manganese-engineered iron oxide nanoparticles through size control. Nanoscale. 2014;6(17):10404–12.
88. Rui Y-P, Liang B, Hu F, Xu J, Peng Y-F, Yin P-H, Duan Y, Zhang C, Gu H. Ultra-large-scale production of ultrasmall superparamagnetic iron oxide nanoparticles for T 1-weighted MRI. RSC Adv. 2016;6(27):22575–85.
89. Zhou Z, Tian R, Wang Z, Yang Z, Liu Y, Liu G, Wang R, Gao J, Song J, Nie L. Artificial local magnetic field inhomogeneity enhances T 2 relaxivity. Nat Commun. 2017;8(1):1–10.

90. Noordin S, Winalski C, Shortkroff S, Mulkern R. Factors affecting paramagnetic contrast enhancement in synovial fluid: effects of electrolytes, protein concentrations, and temperature on water proton relaxivities from Mn ions and Gd chelated contrast agents. Osteoarthr Cartil. 2010;18(7):964–70.
91. Lu C, Dong P, Pi L, Wang Z, Yuan H, Liang H, Ma D, Chai KY. Hydroxyl–PEG–phosphonic acid-stabilized superparamagnetic manganese oxide-doped iron oxide nanoparticles with synergistic effects for dual-mode MR imaging. Langmuir. 2019;35(29):9474–82.
92. Wu L, Zhang Y, Steinberg G, Qu H, Huang S, Cheng M, Bliss T, Du F, Rao J, Song G. A review of magnetic particle imaging and perspectives on neuroimaging. Am J Neuroradiol. 2019;40(2):206–12.
93. Dadfar SM, Camozzi D, Darguzyte M, Roemhild K, Varvarà P, Metselaar J, Banala S, Straub M, Güvener N, Engelmann U. Size-isolation of superparamagnetic iron oxide nanoparticles improves MRI, MPI and hyperthermia performance. J Nanobiotechnol. 2020;18(1):1–13.
94. Lifante J, Shen Y, Ximendes E, Martín Rodríguez E, Ortgies DH. The role of tissue fluorescence in in vivo optical bioimaging. J Appl Phys. 2020;128(17):171101.
95. Loo J F-C, Chien Y-H, Yin F, Kong S-K, Ho H-P, Yong K-T. Upconversion and downconversion nanoparticles for biophotonics and nanomedicine. Coordination Chem Rev. 2019;400:213042.
96. Fan Q, Cui X, Guo H, Xu Y, Zhang G, Peng B. Application of rare earth-doped nanoparticles in biological imaging and tumor treatment. J Biomater Appl. 2020;35(2):237–63.
97. Chen J, Zhao JX. Upconversion nanomaterials: synthesis, mechanism, and applications in sensing. Sensors. 2012;12(3):2414–35.
98. Liang G, Wang H, Shi H, Wang H, Zhu M, Jing A, Li J, Li G. Recent progress in the development of upconversion nanomaterials in bioimaging and disease treatment. J Nanobiotechnol. 2020;18(1):1–22.
99. Chen T, Su L, Ge X, Zhang W, Li Q, Zhang X, Ye J, Lin L, Song J, Yang H. Dual activated NIR-II fluorescence and photoacoustic imaging-guided cancer chemo-radiotherapy using hybrid plasmonic-fluorescent assemblies. Nano Res. 2020;13(12):3268–77.
100. Lo KK-W. Luminescent rhenium (I) and iridium (III) polypyridine complexes as biological probes, imaging reagents, and photocytotoxic agents. Acc Chem Res. 2015;48(12):2985–95.
101. Sheng Z, Cai L. Organic dye-loaded nanoparticles for imaging-guided cancer therapy. Adv Nanotheranost I: Springer; 2016. p. 217–45.
102. Nagahara R, Onda N, Yamashita S, Kojima M, Inohana M, Eguchi A, Nakamura M, Matsumoto S, Yoshida T, Shibutani M. Fluorescence tumor imaging by iv administered indocyanine green in a mouse model of colitis-associated colon cancer. Cancer Sci. 2018;109(5):1638–47.
103. Kaibori M, Matsui K, Ishizaki M, Iida H, Sakaguchi T, Tsuda T, Okumura T, Inoue K, Shimada S, Ohtsubo S. Evaluation of fluorescence imaging with indocyanine green in hepatocellular carcinoma. Cancer Imaging. 2016;16(1):1–7.
104. Zhang C, Jiang D, Huang B, Wang C, Zhao L, Xie X, Zhang Z, Wang K, Tian J, Luo Y. Methylene blue–based near-infrared fluorescence imaging for breast cancer visualization in resected human tissues. Technol Cancer Res Treat. 2019;18:1533033819894331.
105. Choi G, Rejinold NS, Piao H, Choy J-H. Inorganic–inorganic nanohybrids for drug delivery, imaging and photo-therapy: recent developments and future scope. Chem Sci. 2021;
106. Ahmad T, Sarwar R, Iqbal A, Bashir U, Farooq U, Halim SA, Khan A, Al-Harrasi A. Recent advances in combinatorial cancer therapy via multifunctionalized gold nanoparticles. Nanomedicine. 2020;15(12):1221–37.
107. Liu J, Yu M, Zhou C, Yang S, Ning X, Zheng J. Passive tumor targeting of renal-clearable luminescent gold nanoparticles: long tumor retention and fast normal tissue clearance. J Am Chem Soc. 2013;135(13):4978–81.
108. Li D, Liu Y, Yu S, Zhang D, Wang X, Zhong H, He K, Wang Y, Wu Y. Two-photon fluorescence silica nanoparticles-based FRET nanoprobe platform for effectively ratiometric bioimaging of intracellular endogenous adenosine triphosphate. Analyst. 2021.
109. Huang D, He B, Mi P. Calcium phosphate nanocarriers for drug delivery to tumors: imaging, therapy and theranostics. Biomater Sci. 2019;7(10):3942–60.

110. Ashokan A, Gowd GS, Somasundaram VH, Bhupathi A, Peethambaran R, Unni A, Palaniswamy S, Nair SV, Koyakutty M. Multifunctional calcium phosphate nano-contrast agent for combined nuclear, magnetic and near-infrared in vivo imaging. Biomaterials. 2013;34(29):7143–57.
111. Antaris AL, Robinson JT, Yaghi OK, Hong G, Diao S, Luong R, Dai H. Ultra-low doses of chirality sorted (6, 5) carbon nanotubes for simultaneous tumor imaging and photothermal therapy. ACS Nano. 2013;7(4):3644–52.
112. Choi HS, Gibbs SL, Lee JH, Kim SH, Ashitate Y, Liu F, Hyun H, Park G, Xie Y, Bae S. Targeted zwitterionic near-infrared fluorophores for improved optical imaging. Nat Biotechnol. 2013;31(2):148–53.
113. Wang L-W, Peng C-W, Chen C, Li Y. Quantum dots-based tissue and in vivo imaging in breast cancer researches: current status and future perspectives. Breast Cancer Res Treatm. 2015;151(1):7–17.
114. Tholouli E, Sweeney E, Barrow E, Clay V, Hoyland JA, Byers RJ. Quantum dots light up pathology. J Pathol J Pathol Soc Great Br Ireland. 2008;216(3):275–85.
115. Jung S, Chen X. Quantum dot–dye conjugates for biosensing, imaging, and therapy. Adv Healthc Mater. 2018;7(14):1800252.
116. Shen L. Biocompatible polymer/quantum dots hybrid materials: current status and future developments. J Funct Biomater. 2011;2(4):355–72.
117. Kurshanov D, Gromova YA, Cherevkov S, Ushakova E, Kormilina T, Dubavik A, Fedorov A, Baranov A. Non-toxic ternary quantum dots AgInS 2 and AgInS 2/ZnS: synthesis and optical properties. Opt Spectrosc. 2018;125(6):1041–6.
118. Dong J, Wang K, Sun L, Sun B, Yang M, Chen H, Wang Y, Sun J, Dong L. Application of graphene quantum dots for simultaneous fluorescence imaging and tumor-targeted drug delivery. Sensors Actuators B Chem. 2018;256:616–23.
119. Wang H, Mu Q, Wang K, Revia RA, Yen C, Gu X, Tian B, Liu J, Zhang M. Nitrogen and boron dual-doped graphene quantum dots for near-infrared second window imaging and photothermal therapy. Appl Mater Today. 2019;14:108–17.
120. Mehrmohammadi M, Joon Yoon S, Yeager D, Emelianov SY. Photoacoustic imaging for cancer detection and staging. Curr Mol Imaging. 2013;2(1):89–105.
121. De la Zerda A, Zavaleta C, Keren S, Vaithilingam S, Bodapati S, Liu Z, Levi J, Ma T, Oralkan O, Cheng Z. Photoacoustic molecular imaging in living mice utilizing targeted carbon nanotubes. Nature Nanotech. 2008;3:557–62.
122. Han S, Bouchard R, Sokolov KV. Molecular photoacoustic imaging with ultra-small gold nanoparticles. Biomed Opt Express. 2019;10(7):3472–83.
123. Yamada H, Matsumoto N, Komaki T, Konishi H, Kimura Y, Son A, Imai H, Matsuda T, Aoyama Y, Kondo T. Photoacoustic in vivo 3D imaging of tumor using a highly tumor-targeting probe under high-threshold conditions. Sci Rep. 2020;10(1):1–9.
124. Chen Y-S, Frey W, Kim S, Kruizinga P, Homan K, Emelianov S. Silica-coated gold nanorods as photoacoustic signal nanoamplifiers. Nano Lett. 2011;11(2):348–54.
125. Zhang J, Duan F, Liu Y, Nie L. High-resolution photoacoustic tomography for early-stage cancer detection and its clinical translation. Radiol Imaging Cancer. 2020;2(3):e190030.
126. Doan VHM, Nguyen VT, Mondal S, Vo TMT, Ly CD, Vu DD, Ataklti GY, Park S, Choi J, Oh J. Fluorescence/photoacoustic imaging-guided nanomaterials for highly efficient cancer theragnostic agent. Sci Rep. 2021;11(1):1–18.
127. Goel S, England CG, Chen F, Cai W. Positron emission tomography and nanotechnology: a dynamic duo for cancer theranostics. Adv Drug Deliv Rev. 2017;113:157–76.
128. Norregaard K, Jørgensen JT, Simón M, Melander F, Kristensen LK, Bendix PM, Andresen TL, Oddershede LB, Kjaer A. 18F-FDG PET/CT-based early treatment response evaluation of nanoparticle-assisted photothermal cancer therapy. PLoS One. 2017;12(5):e0177997.
129. Narmani A, Farhood B, Haghi-Aminjan H, Mortezazadeh T, Aliasgharzadeh A, Mohseni M, Najafi M, Abbasi H. Gadolinium nanoparticles as diagnostic and therapeutic agents: their

delivery systems in magnetic resonance imaging and neutron capture therapy. J Drug Del Sci Technol Cancer Res Treat. 2018;44:457–66.
130. Maity D, Zoppellaro G, Sedenkova V, Tucek J, Safarova K, Polakova K, Tomankova K, Diwoky C, Stollberger R, Machala L. Surface design of core–shell superparamagnetic iron oxide nanoparticles drives record relaxivity values in functional MRI contrast agents. Chem Commun. 2012;48(93):11398–400.
131. Langereis S, Geelen T, Grüll H, Strijkers GJ, Nicolay K. Paramagnetic liposomes for molecular MRI and MRI-guided drug delivery. NMR Biomed. 2013;26(7):728–44.
132. Kandasamy G, Sudame A, Luthra T, Saini K, Maity D. Functionalized hydrophilic superparamagnetic iron oxide nanoparticles for magnetic fluid hyperthermia application in liver cancer treatment. ACS Omega. 2018;3(4):3991–4005.
133. Kratz H, Eberbeck D, Wagner S, Taupitz M, Schnorr J. Synthetic routes to magnetic nanoparticles for MPI. Biomedizinische Technik/Biomed Eng. 2013;58(6):509–15.
134. Du Y, Lai PT, Leung CH, Pong PW. Design of superparamagnetic nanoparticles for magnetic particle imaging (MPI). Int J Mol Sci. 2013;14(9):18682–710.
135. Mira J G, Potter J L, Fullerton G D, Ezekiel J. Advantages and limitations of computed tomography scans for treatment planning of lung cancer. Intl J Rad Oncol Biol Phys. 1982;8(9):1617–23.
136. Makaju S, Prasad P, Alsadoon A, Singh A, Elchouemi A. Lung cancer detection using CT scan images. Proc Comput Sci. 2018;125:107–14.
137. Jarrett D, Stride E, Vallis K, Gooding MJ. Applications and limitations of machine learning in radiation oncology. Br J Radiol. 2019;92(1100):20190001.
138. Iranmakani S, Mortezazadeh T, Sajadian F, Ghaziani MF, Ghafari A, Khezerloo D, Musa AE. A review of various modalities in breast imaging: technical aspects and clinical outcomes. Egypt J Radiol Nucl Med. 2020;51(1):1–22.
139. Su C, Ren X, Nie F, Li T, Lv W, Li H, Zhang Y. Current advances in ultrasound-combined nanobubbles for cancer-targeted therapy: a review of the current status and future perspectives. RSC Adv. 2021;11(21):12915–28.
140. Guo R, Lu G, Qin B, Fei B. Ultrasound imaging technologies for breast cancer detection and management: a review. Ultrasound Med Biol. 2018;44(1):37–70.
141. Tandale P, Choudhary N, Singh J, Sharma A, Shukla A, Sriram P, Soni U, Singla N, Barnwal R P, Singh G. Fluorescent quantum dots: an insight on synthesis and potential biological application as drug carrier in cancer. Biochem Biophys Rep. 2021;26:100962.
142. Bu L, Shen B, Cheng Z. Fluorescent imaging of cancerous tissues for targeted surgery. Adv Drug Deliv Rev. 2014;76:21–38.
143. Siregar S, Nagoka R, Ishikawa K, Saijo Y. Carbon nanotubes as potential candidate for photoacoustic imaging contrast agent. In: Proceedings of meetings on acoustics 6ICU, Acoustical Society of America. 2017.
144. Zhang R, Wang Z, Xu L, Xu Y, Lin Y, Zhang Y, Sun Y, Yang G. Rational design of a multifunctional molecular dye with single dose and laser for efficiency NIR-II fluorescence/photoacoustic imaging guided photothermal therapy. Anal Chem. 2019;91(19):12476–83.
145. Nyayapathi N, Xia J. Photoacoustic imaging of breast cancer: a mini review of system design and image features. J Biomed Opt. 2019;24(12):121911.
146. Unterrainer M, Eze C, Ilhan H, Marschner S, Roengvoraphoj O, Schmidt-Hegemann N-S, Walter F, Kunz WG, Af Rosenschöld PM, Jeraj R. Recent advances of PET imaging in clinical radiation oncology. Radiat Oncol. 2020;15(1):1–15.
147. Kapoor V, McCook BM, Torok FS. An introduction to PET-CT imaging. Radiographics. 2004;24(2):523–43.
148. Griffeth LK. Use of PET/CT scanning in cancer patients: technical and practical considerations. Taylor & Francis: Baylor University Medical Center Proceedings; 2005.
149. DeVita VT, Chu E. A history of cancer chemotherapy. Cancer Res. 2008;68(21):8643–53.
150. Nichols HJ, Walker JE. Experimental observations on the prophylaxis and treatment of syphilis. J Exp Med. 1923;37(4):525–42.

151. Kumar CS, Mohammad F. Magnetic nanomaterials for hyperthermia-based therapy and controlled drug delivery. Adv Drug Deliv Rev. 2011;63(9):789–808.
152. Périgo EA, Hemery G, Sandre O, Ortega D, Garaio E, Plazaola F, Teran FJ. Fundamentals and advances in magnetic hyperthermia. Appl Phys Rev. 2015;2(4):041302.
153. Maier-Hauff K, Rothe R, Scholz R, Gneveckow U, Wust P, Thiesen B, Feussner A, Von Deimling A, Waldoefner N, Felix R. Intracranial thermotherapy using magnetic nanoparticles combined with external beam radiotherapy: results of a feasibility study on patients with glioblastoma multiforme. J Neuro-Oncol. 2007;81(1):53–60.
154. Carrouée A, Allard-Vannier E, Même S, Szeremeta F, Beloeil J-C, Chourpa I. Sensitive trimodal magnetic resonance imaging-surface-enhanced resonance Raman scattering-fluorescence detection of cancer cells with stable magneto-plasmonic nanoprobes. Anal Chem. 2015;87(22):11233–41.
155. Wang Y, Jiang L, Zhang Y, Lu Y, Li J, Wang H, Yao D, Wang D. Fibronectin-targeting and cathepsin B-activatable theranostic nanoprobe for MR/fluorescence imaging and enhanced photodynamic therapy for triple negative breast cancer. ACS Appl Mater Interf. 2020;12(30):33564–74.
156. Dougherty TJ, Gomer CJ, Henderson BW, Jori G, Kessel D, Korbelik M, Moan J, Peng Q. Photodynamic therapy. JNCI. 1998;90(12):889–905.
157. Chen J, Keltner L, Christophersen J, Zheng F, Krouse M, Singhal A, Wang S-S. New technology for deep light distribution in tissue for phototherapy. Cancer J. 2002;8(2):154–63.
158. Brown SB, Brown EA, Walker I. The present and future role of photodynamic therapy in cancer treatment. Lancet Oncol. 2004;5(8):497–508.
159. Josefsen L B, Boyle R W. Photodynamic therapy and the development of metal-based photosensitisers. Metal-Based Drugs. 2008; 2008.
160. Allison RR, Downie GH, Cuenca R, Hu X-H, Childs CJ, Sibata C. Photosensitizers in clinical PDT. Photodiag Photodyn Ther. 2004;1(1):27–42.
161. Huang Z. A review of progress in clinical photodynamic therapy. Technol Cancer Res Treat. 2005;4(3):283–93.
162. O'Connor AE, Gallagher WM, Byrne AT. Porphyrin and nonporphyrin photosensitizers in oncology: preclinical and clinical advances in photodynamic therapy. Photochem Photobiol. 2009;85(5):1053–74.
163. Foster TH, Pearson BD, Mitra S, Bigelow CE. Fluorescence anisotropy imaging reveals localization of meso-tetrahydroxyphenyl chlorin in the nuclear envelope. Photochem Photobiol. 2005;81(6):1544–7.
164. Wilson JD, Bigelow CE, Calkins DJ, Foster TH. Light scattering from intact cells reports oxidative-stress-induced mitochondrial swelling. Biophys J. 2005;88(4):2929–38.
165. Mellish KJ, Cox RD, Vernon DI, Griffiths J, Brown SB. In vitro photodynamic activity of a series of methylene blue analogues. Photochem Photobiol. 2002;75(4):392–7.
166. Swartling J, Höglund OV, Hansson K, Södersten F, Axelsson J, Lagerstedt A-S. Online dosimetry for temoporfin-mediated interstitial photodynamic therapy using the canine prostate as model. J Biomed Opt. 2016;21(2):028002.
167. Swartling J, Axelsson J, Ahlgren G, Kälkner KM, Nilsson S, Svanberg S, Svanberg K, Andersson-Engels S. System for interstitial photodynamic therapy with online dosimetry: first clinical experiences of prostate cancer. J Biomed Opt. 2010;15(5):058003.
168. Huang X, El-Sayed IH, Qian W, El-Sayed MA. Cancer cell imaging and photothermal therapy in the near-infrared region by using gold nanorods. J Am Chem Soc. 2006;128(6):2115–20.
169. Huang X, El-Sayed MA. Gold nanoparticles: optical properties and implementations in cancer diagnosis and photothermal therapy. J Adv Res. 2010;1(1):13–28.
170. Hauck TS, Jennings TL, Yatsenko T, Kumaradas JC, Chan WC. Enhancing the toxicity of cancer chemotherapeutics with gold nanorod hyperthermia. Adv Mater. 2008;20(20):3832–8.
171. Huang X, Jain PK, El-Sayed IH, El-Sayed MA. Plasmonic photothermal therapy (PPTT) using gold nanoparticles. Lasers Med Sci. 2008;23(3):217–28.
172. Loo C, Lowery A, Halas N, West J, Drezek R. Immunotargeted nanoshells for integrated cancer imaging and therapy. Nano Lett. 2005;5(4):709–11.

173. Abbasi A, Park K, Bose A, Bothun G. Near-infrared responsive gold–layersome nanoshells. Langmuir. 2017;33(21):5321–7.
174. Zou L, Wang H, He B, Zeng L, Tan T, Cao H, He X, Zhang Z, Guo S, Li Y. Current approaches of photothermal therapy in treating cancer metastasis with nanotherapeutics. Theranostics. 2016;6(6):762.
175. Thorat ND, Bohara RA, Yadav HM, Tofail SA. Multi-modal MR imaging and magnetic hyperthermia study of Gd doped Fe_3O_4 nanoparticles for integrative cancer therapy. RSC Adv. 2016;6(97):94967–75.
176. Torigian DA, Zaidi H, Kwee TC, Saboury B, Udupa JK, Cho Z-H, Alavi A. PET/MR imaging: technical aspects and potential clinical applications. Radiology. 2013;267(1):26–44.
177. Yanli W, Xianzhu X, Qianlan L, Ruchun Y, Haixin D, Qiang X. Synthesis of bifunctional Gd2O3: Eu3+ nanocrystals and their applications in biomedical imaging. J Rare Earths. 2015;33(5):529–34.
178. Li M, Fang H, Liu Q, Gai Y, Yuan L, Wang S, Li H, Hou Y, Gao M, Lan X. Red blood cell membrane-coated upconversion nanoparticles for pretargeted multimodality imaging of triple-negative breast cancer. Biomater Sci. 2020;8(7):1802–14.
179. Tang H, Wang M, Meng C, Tao W, Wang C, Yu H. Research on design, fabrication, and properties of Fe_2O_3@ SiO_2/CDs/PEG@ $nSiO_2$ nanocomposites. Materials Letters. 2019; 235:39–41.
180. Lee J, Hwang G, Hong YS, Sim T. One step synthesis of quantum dot–magnetic nanoparticle heterodimers for dual modal imaging applications. Analyst. 2015;140(8):2864–8.
181. Boase NR, Blakey I, Rolfe BE, Mardon K, Thurecht K. Synthesis of a multimodal molecular imaging probe based on a hyperbranched polymer architecture. Polym Chem. 2014;5(15):4450–8.
182. Lee C-M, Cheong S-J, Kim E-M, Lim ST, Jeong YY, Sohn M-H, Jeong H-J. Nonpolymeric surface–coated iron oxide nanoparticles for in vivo molecular imaging: biodegradation, biocompatibility, and multiplatform. J Nucl Med. 2013;54(11):1974–80.
183. Ge J, Jia Q, Liu W, Lan M, Zhou B, Guo L, Zhou H, Zhang H, Wang Y, Gu Y. Carbon dots with intrinsic theranostic properties for bioimaging, red-light-triggered photodynamic/photothermal simultaneous therapy in vitro and in vivo. Adv Healthc Mater. 2016;5(6):665–75.
184. Dai L, Zhang Q, Li J, Shen X, Mu C, Cai K. Dendrimerlike mesoporous silica nanoparticles as pH-responsive nanocontainers for targeted drug delivery and bioimaging. ACS Appl Mater Interf. 2015;7(13):7357–72.
185. Sun Q, You Q, Wang J, Liu L, Wang Y, Song Y, Cheng Y, Wang S, Tan F, Li N. Theranostic nanoplatform: triple-modal imaging-guided synergistic cancer therapy based on liposome-conjugated mesoporous silica nanoparticles. ACS Appl Mater Interf. 2018;10(2):1963–75.
186. Yang Z, Fan W, Zou J, Tang W, Li L, He L, Shen Z, Wang Z, Jacobson O, Aronova MA. Precision cancer theranostic platform by in situ polymerization in perylene diimide-hybridized hollow mesoporous organosilica nanoparticles. J Am Chem Soc. 2019;141(37):14687–98.
187. Langbein T, Weber WA, Eiber M. Future of theranostics: an outlook on precision oncology in nuclear medicine. J Nucl Med. 2019;60(Suppl 2):13S–9S.